

Generation of a Zn²⁺-free oxygenase of phenol hydroxylase from

Pseudomonas sp. strain CF600

Natalie Khor

A Thesis

in

The Department

of

Chemistry and Biochemistry

Presented in partial Fulfillment of the Requirements

for the Degree of Master of Science at

Concordia University

Montreal, Quebec, Canada

April 2014

© Natalie Khor, 2014

CONCORDIA UNIVERSITY
School of Graduate Studies

This is to certify that the thesis prepared

By: Natalie Khor _____

Entitled: Generation of a Zn²⁺-free oxygenase of phenol hydroxylase from *Pseudomonas* sp. strain CF600

and submitted in partial fulfillment of the requirements for the degree of
MASTER OF SCIENCE (Chemistry)

complies with the regulations of the University and meets the accepted standards with respect to originality and quality.

Signed by the final examining committee:

Dr. M.J. Kornblatt _____ Chair

Dr. P. Joyce _____ Examiner

Dr. J. Turnbull _____ Examiner

Dr. J. Powlowski _____ Supervisor

Approved by _____
Chair of Department or Graduate Program Director

Dean of Faculty

Date _____

ABSTRACT

Generation of a Zn²⁺-free oxygenase of phenol hydroxylase from

Pseudomonas sp. strain CF600

Natalie Khor

The phenol hydroxylase enzyme from *Pseudomonas* sp. strain CF600 is involved in the conversion of phenol to catechol, which subsequent enzymes break down to precursors for the Krebs cycle. The protein is a multi-component enzyme that is composed of reductase (DmpP), oxygenase (DmpLNO dimer), activator (DmpM) and assembly (DmpK) subunits. The active site, found in DmpN of the oxygenase component, has a binuclear iron centre required for activity. In DmpN, previous experiments have shown that there is also a Zn²⁺ ion coordinated by four cysteine residues, but the role that it plays in the enzyme has yet to be elucidated.

Site-directed mutagenesis was previously performed on two of the cysteine ligands in DmpN (C433A and C437A) that form a complex with Zn²⁺, but attempts to express and purify the variant proteins were unsuccessful. In this thesis, different techniques were used to attempt removal of Zn²⁺ from its binding site in the oxygenase. These techniques included dialysis and column buffer exchange in the presence of a combination of chelating agents, ethylenediaminetetraacetic acid (EDTA) or tetrakis-(2-pyridylmethyl) ethylenediamine (TPEN), reducing agents dithiothreitol (DTT) or tris(2-carboxyethyl)phosphine (TCEP) and a denaturant, urea. Protein samples were analysed with circular dichroism and fluorescence spectroscopy for secondary and tertiary structure changes, respectively. In addition, inductively-coupled plasma mass spectrometry (ICP-MS) was used to determine the metal content of the treated proteins.

The most successful approach was the combination of TPEN, DTT and urea followed by dialysis against metal-free buffer, where Zn^{2+} was reduced from 2.6 atoms per molecule in pre-dialysis to 0.1 atoms per molecule after dialysis. This treatment, however, also resulted in the removal of Fe^{2+} from the enzyme. The method developed for the preparation of the apo-enzyme will enable further experiments to investigate the roles of metal ions in this enzyme following their controlled re-insertion.

ACKNOWLEDGEMENTS

First and foremost, I would like to thank my supervisor Dr. Justin Powlowski for his patience, endless guidance and support throughout my Master's studies. His advices and insights, which have always been greatly appreciated, have taught me to think and grow a bit at a time to become a more critical researcher. His careful editing has contributed immensely to the completion of this thesis.

Secondly, I would like to thank my committee members, Dr. Paul Joyce and Dr. Joanne Turnbull, for the time they took to listen and give thoughtful feedbacks and suggestions for my project.

I would like to specially thank Dr. Jack Kornblatt for his generosity in allowing me to use his fluorimeter and Alain Tessier for the ICP-MS analysis and the times he spent to explain any questions I had regarding the instrument.

My wonderful lab mates who have been ever-so encouraging and supportive: Racha, Ekwe and Mark-Anthony, I thank them for their friendship and kindness, and Dr. Sahlman, Liz and Yu Lei for their willingness to help and give suggestions whenever I needed it.

Lastly I would like to thank my parents, brother, Sharon, Lyly and Hayline for their love, encouragement and being the pillars of support throughout this journey.

LIST OF FIGURES

Figure 1.1 <i>Meta</i> -cleavage pathway for phenol degradation.....	4
Figure 1.2 <i>Ortho</i> -cleavage pathway for phenol degradation.....	4
Figure 2. Schematic of dmp operon encoding 15 genes for phenol hydroxylase and <i>meta</i> -cleavage pathway from <i>Pseudomonas</i> sp. strain CF600.....	7
Figure 3. Quaternary structure of PHH and PHM from <i>Pseudomonas</i> sp. OX1	10
Figure 4. Zn ²⁺ -binding site on α -subunit of PHH of phenol hydroxylase from <i>Pseudomonas</i> sp. OX1	11
Figure 5. Sequence alignment of <i>Pseudomonas</i> sp. CF600 DmpN and <i>Pseudomonas</i> sp. OX1 PHH α -subunit.....	12
Figure 6. Structure of metal chelators used in this study.....	15
Figure 7. SDS-PAGE (12%) gel electrophoresis of C436A variant protein expressed at 18 °C for 48 h under induced (with IPTG) and uninduced conditions.....	27
Figure 8. Circular dichroism studies of native oxygenase.....	29
Figure 9. Intrinsic fluorescence spectra of native oxygenase as a function of temperature.....	31
Figure 10. Far-UV CD spectra of EDTA and EDTA/DTT treated samples pre- and post-dialysis.....	37
Figure 11. Intrinsic fluorescence of EDTA and EDTA/DTT-treated oxygenase pre- and post-dialysis as a function of temperature.....	38
Figure 12. CD spectra and thermal denaturation curves of pre- and post-dialysis TCEP and TCEP/EDTA-treated oxygenase samples.....	41
Figure 13. Intrinsic fluorescence intensity of TCEP- and TCEP/EDTA treated oxygenase samples pre- and post-dialysis.....	43
Figure 14. Circular dichroism spectra of native oxygenase incubated with varying concentrations of urea.....	45
Figure 15. Far-UV CD spectra of EDTA-treated and EDTA/DTT-treated oxygenase after metal-free buffer column exchange with NAP-5.....	49
Figure 16. Intrinsic fluorescence monitored denaturation of EDTA and EDTA/DTT-treated-oxygenase desalted using a NAP-5 metal-free buffer exchange column.....	50
Figure 17. Far-UV CD spectra of TPEN/DTT/urea-treated oxygenase before and after dialysis.....	53
Figure 18. Intrinsic fluorescence to monitor denaturation of TPEN/DTT/urea-treated oxygenase, pre- and post-dialysis.....	54

LIST OF TABLES

Table 1. ICP-MS metal analysis of iron and zinc in native oxygenase protein.	33
Table 2. ICP-MS analysis of iron and zinc in DTT-treated oxygenase before and after dialysis.....	35
Table 3. ICP-MS metal analysis of iron and zinc in oxygenase protein samples..	39
Table 4. ICP-MS metal analysis of iron and zinc in TCEP- and TCEP/EDTA-treated oxygenase pre- and post-dialysis.	44
Table 5. ICP-MS metal analysis of EDTA/DTT and urea-treated oxygenase before and after dialysis.....	47
Table 6. ICP-MS metal analysis of EDTA- and EDTA/DTT-treated oxygenase after NAP-5 column purification.....	48
Table 7. ICP-MS metal analysis of TPEN and DTT-treated oxygenase in the presence or absence of urea, before and after dialysis.....	52
Table 8. ICP-MS metal analysis of DTT-treated oxygenase in the presence or absence of EDTA, TPEN and urea after Chelex® treatment.	55

TABLE OF CONTENTS

LIST OF FIGURES	vi
LIST OF TABLES	vii
LIST OF ABBREVIATIONS	x
INTRODUCTION	1
General Introduction	1
Phenol in the Environment.....	2
Phenol Degrading Bacteria and Their Metabolic Pathways	3
<i>Pseudomonas</i> sp. strain CF600	6
Reductase Component - DmpP	6
Activator Component - DmpM.....	7
Oxygenase Component - DmpLNO.....	8
Assembly Component - DmpK.....	8
Structure of Phenol Hydroxylase in <i>Pseudomonas</i> sp. OX1.....	9
Roles of Zn ²⁺ in Enzymes	13
Catalytic Roles of Zn ²⁺ in Enzymes	13
Structural Role of Zn ²⁺	14
Zn ²⁺ Chelators	14
Specific Objectives	16
MATERIALS AND METHODS.....	18
Materials	18
SDS-PAGE	18
Protein Concentration Estimation	19
Bacterial Growth and DmpLNO Expression	19
Crude Extract Preparation for Purification of DmpLNO.....	20
Purification of Phenol Hydroxylase DmpLNO.....	20
Phenol Hydroxylase Activity Assay	22
Apo-oxygenase Preparation	22
Liquid Chromatography Inductively-Coupled Plasma Mass Spectrometry (LC-ICP-MS) Analysis	23
Spectroscopic Analysis	24
Generation of Fluorescence Intensity and Wavelength Graphs.....	25

Estimation of T _m values	25
RESULTS	26
Wild-Type Oxygenase Purification from <i>Pseudomonas</i> sp. CF600	26
Variant Oxygenase Protein C433A & C437A Expression at 18 °C and 37 °C	26
Variant Oxygenase Protein C436A Expressed at 18 °C with Addition of Zn ²⁺	26
Alternative Strategy to Characterize the Zn ²⁺ Binding Site	28
Structure Stability of the Native Oxygenase Probed Using Circular Dichroism and Fluorescence Spectroscopies.....	29
Metal Content in Native Oxygenase	32
Overview of the Zn ²⁺ -Chelating Experiments	34
Metal Analysis of DTT-Treated Oxygenase.....	34
Spectroscopic Analysis of Oxygenase Treated with EDTA and DTT.....	35
Metal Analysis of EDTA-Treated Samples	39
Spectroscopic Analysis of TCEP-Treated Oxygenase in the Presence and Absence of EDTA	39
Metal Content in Oxygenase after TCEP Treatment	44
Effects of Urea on the CD Spectra of Native Oxygenase	44
Metal Content of Urea-Treated Oxygenase in the Presence of EDTA and DTT.....	46
Metal Analysis of EDTA- and EDTA/DTT-Treated Oxygenase after Column Buffer Exchange	47
Temperature Denaturation of Samples Prepared Using the NAP-5 Column.....	48
Metal Analysis of TPEN-Treated Oxygenase in the Presence of a Combination of DTT and/or Urea..	51
Temperature Denaturation of TPEN-Treated Oxygenase.....	52
Metal Analysis of Oxygenase after Mini-Chelex [®] Purification.....	54
DISCUSSION	56
CONCLUSIONS.....	64
FUTURE WORK.....	65
REFERENCES	66

LIST OF ABBREVIATIONS

BCA, bicinchoninic acid

BS³, bis(sulfosuccinimidyl)suberate

CD, circular dichroism

DTT, dithiothreitol

Dmp, dimethyl phenol

DNaseI, deoxyribonuclease I

EDC, 1-ethyl-3-[3-(dimethylamino)propyl]carbodiimide hydrochloride

EDTA, ethylenediaminetetraacetic acid

GdHCl, guanidine hydrochloride

FAD, flavin adenine dinucleotide

IPTG, isopropyl β -D-1-thiogalactopyranoside

LC-ICP-MS, liquid chromatography inductively-coupled plasma mass spectrometry

LD₅₀, lethal dose to kill 50% of population

NADH, nicotinamide adenine dinucleotide

PAGE, polyacrylamide gel electrophoresis

TCA, trichloroacetic acid

TCA cycle, tricarboxylic acid cycle

TCEP, tris(2-carboxyethyl)phosphine

T_m, transition midpoint temperature

TPEN, tetrakis-(2-pyridylmethyl) ethylenediamine

Tris, tris(hydroxymethyl)aminomethane

INTRODUCTION

General Introduction

In the mid-eighteenth century, when the Industrial Revolution had just begun, many manufacturing plants were created and as a result chemical waste production increased. Phenol, an aromatic compound, along with its derivatives, is now produced in amounts of millions of kilograms per year from industrial sources such as oil refineries, pulp and paper, pesticide production, textiles and pharmaceutical¹. Some phenolic waste finds its way into the environment. As phenol is toxic to humans and other organisms, this can contribute to environmental pollution if it is not degraded or removed.

Humans have very limited ability to completely degrade aromatic compounds. The three aromatic amino acids, phenylalanine, tyrosine and tryptophan, are some of the few that can be converted to Krebs cycle and glycolytic intermediates. When an aromatic xenobiotic such as phenol enters the human system, it is prepared for excretion in two steps: hydroxylation through cytochrome P-450 in the liver, and/or conjugation (glucuronidation or sulfation). The addition of polar groups renders phenol more water soluble so that it is more readily excreted.²

Toxicity testing on animals such as mice and rabbits has been performed to determine the LD₅₀ (lethal dose which is required to kill 50% of the population) of phenol. The Agency for Toxic Substances and Disease Registry (ATSDR) in the United States and Health Canada have compiled information on studies from research papers reporting tests on animals that were administered phenol orally and dermally. The LD₅₀ value for mice and rabbits given phenol orally ranged between 0.34 – 0.65 g/kg body weight^{3,4}. Dermal exposure of rats to phenol gave a similar LD₅₀ range of 0.5 – 0.68 g/kg body weight compared to that of oral ingestion^{5,6}.

Phenol in the Environment

To remove pollutants such as phenol and its derivatives from chemical wastes or the environment, various physicochemical methods can be used: adsorption, oxidation, membrane separation and reverse osmosis.⁷ These methods, however, have limitations, are expensive when used to treat large amounts (for example, of soil or water), and in the process they can produce other toxic compounds.⁸ Incineration is another technique that is used when disposal of phenol is required.⁹ Electrochemical incineration of phenol and its derivatives is gaining popularity with the development of electrodes that are effective at decomposing these compound, producing carbon dioxide and water.¹⁰

Bioremediation is an alternative method of environmental or waste clean-up. This involves using microorganisms to remove, from soil or water, phenolic compounds such as herbicides used in agriculture, or industrial waste, that are expelled into the environment.¹¹ Over the course of time, bacteria and fungi growing in surroundings rich in aromatic compounds have acquired the ability to degrade chemicals such as phenol to carbon dioxide and water. They do so by using enzymes such as hydroxylases and dioxygenases to form catechol, which can be cleaved in the presence of oxygen, and further broken down to smaller molecules that these organisms use as sources of carbon and energy.

The types of chemical groups, their positions (*ortho*, *meta* or *para*), and the number of substituents on the benzene ring govern the rate at which microorganisms breakdown an aromatic compound. These conjugated ring system compounds, such as phenol or benzoic acid, that are substituted with hydroxyl or carboxyl groups can be easily degraded by microbes, whereas halide, sulfonate or nitro groups positioned on a benzene ring create a bigger challenge

for microbial decomposition. For example, a study showed that regardless of position on the ring with respect to a hydroxyl or carboxyl group, a halogenated compound was degraded in less than two weeks as opposed to one or two days without the halogen¹². The position and number of chlorine substituents on the ring also affect the degradation rate: for example, *o*- and *p*-chlorobenzoate are degraded faster than *m*-chlorobenzoate, and the more substituents there are, the less susceptibility to microbial degradation¹³ there is. Longer aliphatic side chains on the benzene ring result in a slower rate of biodegradation compared to shorter chains, as shown by studies of aromatic herbicide degradation¹⁴. Cresols also require extra steps to be fully degraded by microorganisms. The methyl group on a cresol is either oxidized such that subsequent reactions allow it to be converted to catechol before it gets further degraded¹⁵, or the ring is oxidized to form a catechol with a methyl group that will eventually undergo *meta*-fission¹⁶.

Phenol Degrading Bacteria and Their Metabolic Pathways

There are two pathways by which bacteria catabolize phenol after it is converted to catechol by a monooxygenase, characterized by whether addition of oxygen to the ring results in *meta*- or *ortho*-cleavage. In an *ortho*-cleavage pathway, catechol is cleaved by action of the enzyme catechol 1,2-dioxygenase, which inserts molecular oxygen into the ring between two hydroxyl substituents generating a non-aromatic dicarboxylic acid product (reviewed in Ornston & Yeh 1982)¹⁷. *Meta*-cleavage of a catechol ring occurs between a hydroxyl group and an adjacent carbon that is not hydroxylated, generating a non-aromatic semialdehyde product (reviewed in Bayly & Barbour 1984).¹⁷ Figures 1.1 and 1.2, show the pathways subsequent to ring cleavage. The final products of the *meta*-cleavage pathway for catechol are pyruvate and acetyl-CoA, both of which are fed into the tricarboxylic acid cycle (TCA cycle)¹⁷. On the other

hand, the *ortho*-cleavage pathway for catechol ultimately results in the production of acetyl-CoA and succinate²².

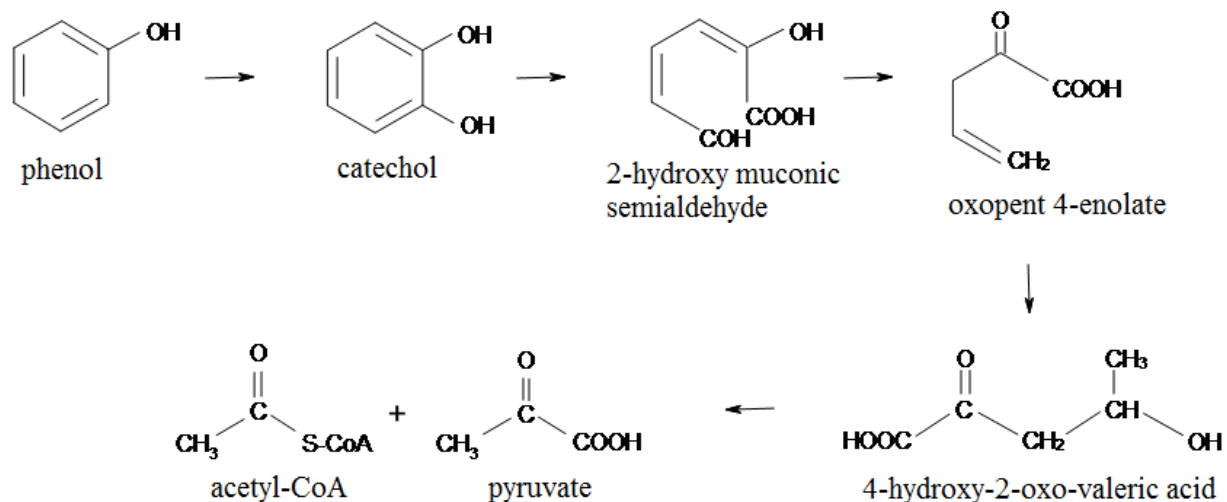


Figure 1.1 *Meta*-cleavage pathway for phenol degradation. Permission to reprint and redraw obtained from publisher. (17)

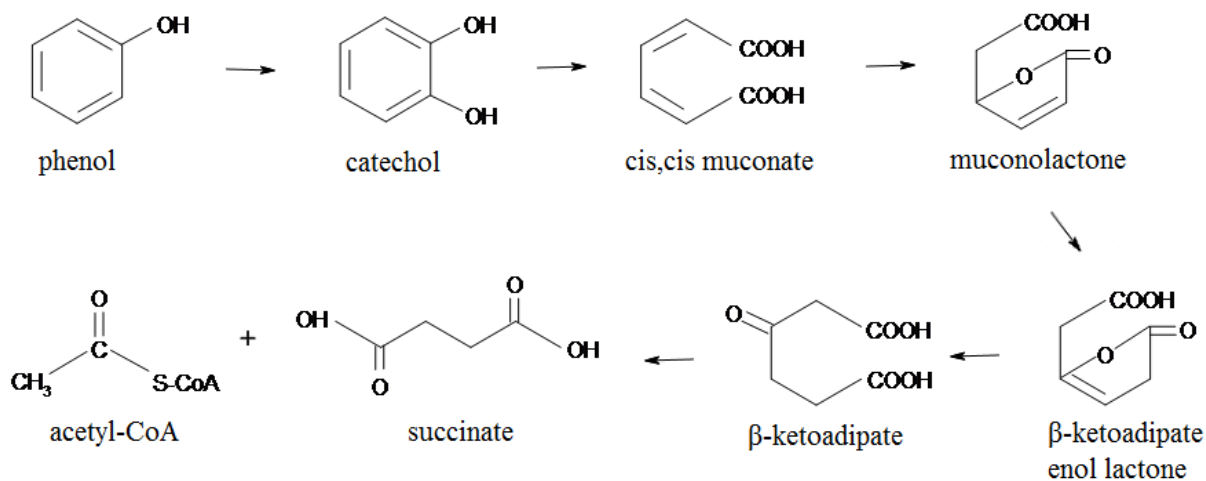


Figure 1.2 *Ortho*-cleavage pathway for phenol degradation. Permission to reprint and redraw obtained from publisher. (22)

The *meta*-cleavage pathway in the degradation of phenol is common in many pseudomonads including *Pseudomonas sp.* CF600, which is the subject of this thesis. Some species, such as *Pseudomonas putida*, can have both *meta*- and *ortho*-cleavage depending on the starting carbon source: benzoate is degraded via *ortho* ring cleavage whereas phenols and cresols are degraded via a *meta*-cleavage pathway¹⁸. Examples of non-pseudomonads that also have *meta*-cleavage pathways are *Azotobacter vinelandii* 206¹⁹ and *Alcaligenes eutrophus*²⁰.

Cleavage of catechol via the *ortho*-cleavage pathway leads to degradation of this aromatic compound but results in different precursors for the TCA cycle than the *meta*-cleavage pathway. A well-studied organism that uses the *ortho* ring fission pathway for phenol degradation via catechol is the yeast species, *Trichosporon cutaneum*. When grown on phenol as the sole carbon source, hydroxylation of phenol forms catechol, and catechol 1,2-oxygenase cleaves the bond between the hydroxyl groups to generate *cis,cis*-muconate²¹ (Fig. 1.2). Further studies confirmed that the β -keto adipate pathway then follows and ultimately results in formation of succinate and acetyl-CoA as precursors for the Krebs cycle^{22, 23} (Fig. 1.2). Purification and characterization of the phenol hydroxylase enzyme from *T. cutaneum* showed that it is a monomer of 148 kDa and contains FAD; it is not a multi-subunit protein²⁴. Another yeast, *Candida tropicalis*, can degrade phenols, resorcinol and quinol using *ortho* ring fission but cannot decompose benzoates, cresols and other derivatives of phenol, unlike *T. cutaneum*²⁵.

Bacterial species that use *ortho*-cleavage for aromatic degradation are also known, although the range of bacterial species is not as extensive as those using *meta*-cleavage²⁶. One of the pioneering studies of the β -keto adipate pathway was using the bacterial species *Pseudomonas putida*, which uses catechol and protocatechuate and converts them to β -

ketoacid^{27,28,29,30}. *Streptomyces setonii*, another bacterial species, was the first strain of the *Streptomyces* genus reported to undertake phenol degradation using an *ortho*-cleavage pathway³¹.

***Pseudomonas* sp. strain CF600**

One of the bacteria most-studied in the degradation of phenols is *Pseudomonas* sp. strain CF600, which is capable of degrading phenol and methyl-substituted phenols using the *meta*-cleavage pathway. The *dmp* operon of *Pseudomonas* sp. strain CF600 contains 15 genes *dmpKLMNOPQBCDEFGHI* that encode proteins involved in phenol hydroxylation and *meta*-cleavage, as shown in Fig 2.¹⁷ The five genes, *dmpLMNOP*, downstream of the regulatory gene, *dmpR*, encode the multi-component enzyme phenol hydroxylase, which is involved in the hydroxylation of phenol to catechol. The five encoded subunits cluster into three components: a reductase (DmpP), an activator (DmpM) and oxygenase (DmpLNO).

Reductase Component - DmpP

DmpP is a 39 kDa protein³², containing an FAD prosthetic group and an iron-sulfur centre that plays a role in the delivery of electrons from NADH to the oxygenase.³³ The FAD cofactor is the redox center of the DmpP protein and is responsible for accepting electrons from NADH and transferring them via the iron-sulfur cluster to the oxygenase component, DmpLNO.³⁴

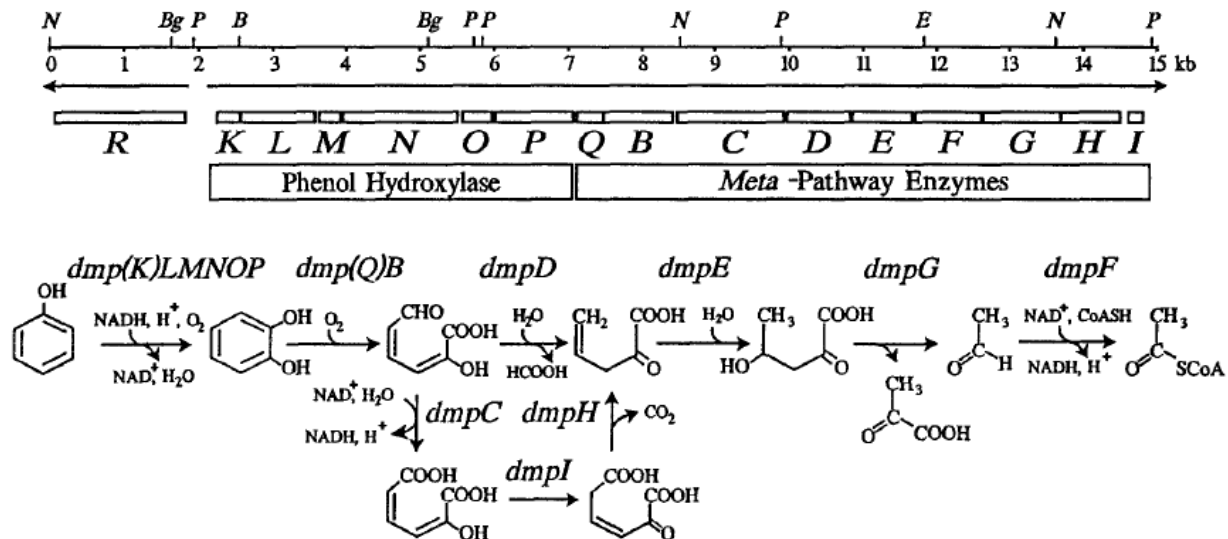


Figure 2. Schematic of *dmp* operon encoding 15 genes for phenol hydroxylase and meta-cleavage pathway enzymes from *Pseudomonas* sp. strain CF600. Obtained permission to reprint from publisher (17).

Activator Component - DmpM

DmpM is a small protein of 10 kDa³³ containing no prosthetic groups and is required for a fully functional phenol hydroxylase enzyme.³⁵ Single turnover experiments from the oxygenase of phenol hydroxylase observed lower product yield in the absence of DmpM compared to in the presence of this component, indicating that its role is to enhance the rate of product yield of the oxygenase component. Previous chemical cross-linking experiments using 1-ethyl-3-[3-dimethylaminopropyl]carbodiimide (EDC) as a cross-linker have shown that DmpM interacts with DmpN and DmpLN of the oxygenase component, although the mechanism for how this occurs has yet to be determined³⁵.

Oxygenase Component - DmpLNO

The oxygenase component of phenol hydroxylase (DmpLNO) forms a dimer of the three subunits. The molecular masses of DmpL, DmpN and DmpO are 34 kDa, 58 kDa and 13 kDa, respectively³³. The active site of the enzyme is found in the DmpN subunit and contains a diiron center thought to be responsible for oxygen activation: reduced DmpLNO in the presence of DmpM can turnover to produce catechol³⁴. Without the presence of iron in the oxygenase, the enzyme is inactive. Previous ICP-MS studies of recombinant enzyme in *E. coli* expressed without addition of iron have shown that iron content in oxygenase was 1.4 per monomer of DmpN and zinc content was also determined to be 0.7 per monomer³⁵.

Assembly Component - DmpK

Although the gene encoding DmpK, the assembly component with a molecular mass of 12.5 kDa³³, is contiguous with the set of genes that encodes phenol hydroxylase, it is not required for oxygenase activity.³⁶ Experiments using bis(sulfosuccinimidyl)suberate (BS³) as a cross-linker have shown that DmpK interacts with DmpL and DmpN of the oxygenase.³⁶ At low concentrations of DmpK, it was shown to obstruct the interaction between DmpM and DmpLNO, and decrease turnover of substrate to products, as evident from activity assays³⁶. Interestingly, at low ferrous concentrations, DmpK appears to facilitate iron incorporation into the apo-enzyme and render the oxygenase functional^{Error! Bookmark not defined.}. This observation suggested that the role of DmpK is to incorporate iron into apo-oxygenase when the concentration of iron is limiting, and hence DmpK may be considered to be an assembly component^{Error! Bookmark not defined.}.

Structure of Phenol Hydroxylase in *Pseudomonas* sp. OX1

The structure of phenol hydroxylase in *Pseudomonas* sp. strain CF600 has yet to be elucidated, but it has 79% DmpN, 62% DmpL and 54% DmpO sequence identity to the α -, β - and γ -subunits, respectively, of phenol hydroxylase from *Pseudomonas* sp. OX1. The X-ray crystal structure of this hydroxylase, PHH ($\alpha\beta\gamma$)₂, in complex with its regulatory protein, PHM (corresponding to DmpM), has been determined³⁷ (Fig. 3). As is evident from Fig. 3, PHM complexes with PHH just above the diiron centre. Since PHH is a dimer, there is one diiron centre in each α -subunit of the protein which is also the largest hydroxylase subunit, totalling four iron atoms. A zinc ion binding site is also present in each α -subunit. The zinc atom is coordinated by four cysteine residues (C399, C402, C432 and C436), as shown in Fig. 4. Sequence alignment of the CF600 and OX1 subunits (Fig. 5) have shown that the cysteine residues are conserved in the Zn²⁺ binding site, but the position of the cysteines are shifted one residue in DmpN. The Zn²⁺ binding site is located at the C-terminal domain of the α -subunit of PHH and has been postulated to be involved in stabilizing that domain³⁷.

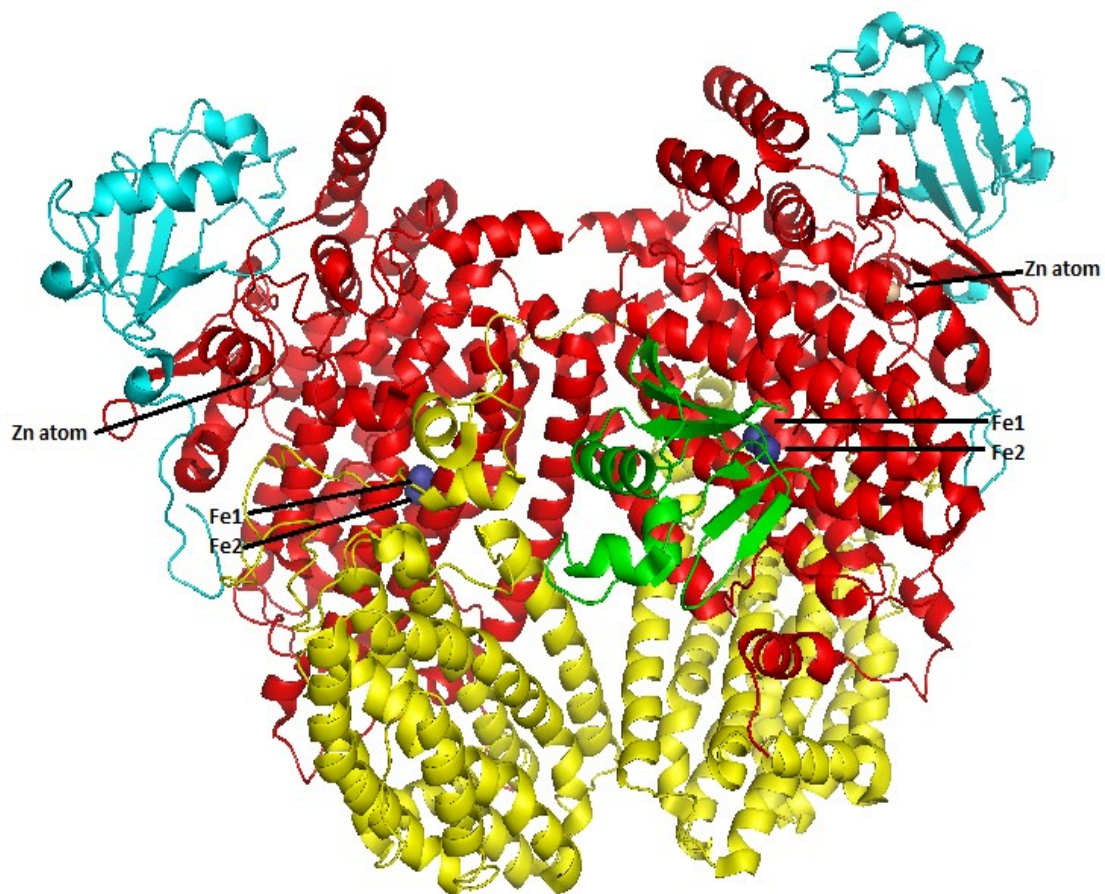


Figure 3. Quaternary structure of PHH and PHM from *Pseudomonas sp. OX1* β -subunit of PHH (yellow), PHM (green), α -subunit of PHH (red), γ -subunit of PHH (cyan), iron atoms (dark blue spheres), zinc atoms (grey spheres). Generated from PyMol Version 1.00, PDB ID: 2INN.

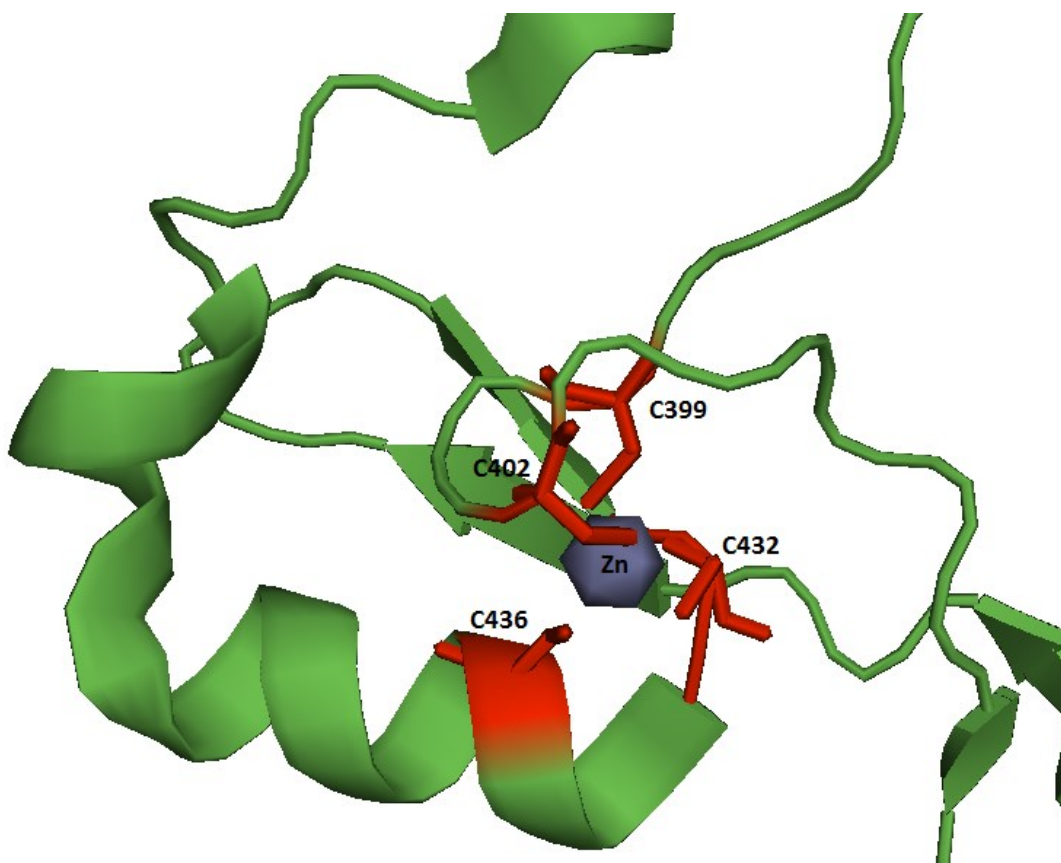


Figure 4. Zn^{2+} -binding site on α -subunit of PHH of phenol hydroxylase from *Pseudomonas sp. OX1*. The zinc atom is coordinated by four cysteine residues (C399, C402, C432 and C436) at the C-terminal domain of α -subunit of PHH. Generated from PyMol Version 1.00, PDB ID: 2INN.

DmpN	YRYLTRDLAWETTYQKKEDVFPLEHFEGIKITDWDKWEDPFRLTMDTYWKYQAEKEKKLY	74
α -subunit	YQYLTRDMAWEPTYQDKKDIPEEDFEGIKITDWSQWEDPFRLTMDAYWKYQAEKEKKLY	73
DmpN	AIFDAFAQNNGHQNISDARYVNALKLFLTAVSPLYEQAFQGF SRVGRQFSGAGARVACQM	134
α -subunit	AIFDAFAQNNGHQNISDARYVNALKLFISGISPLEHAAFQGYSKVGRQFSGAGARVACQM	133
DmpN	QAIDELRHVQTQVHAMSHYNKHF DGLHDFAHMYDRVWYLSVPKSYMDDARTAGPF EFLTA	194
α -subunit	QAIDELRHSQTQQHAMSHYNKHF NGLHDGPHMHRVWYLSVPKSFDDARSAGPF EFLTA	193
DmpN	VSFSEFYVLTNLLFVPPFMSGAA YNGDMATVTFGFSAQSDEARHMTLGLEVIKFMLEQHED	254
α -subunit	ISFSFEYVLTNLLFVPPFMSGAA YNGDMATVTFGFSAQSDEARHMTLGLEVIKFILEQHED	253
DmpN	NVPIIQRWIDKWFWRGYRLLTLIGMMMDYMLPNKVMWSWSEAWGVYFEQAGGALFKDLERY	314
α -subunit	NVPIVQRWIDKWFWRGFRLLSLVSMMDYMLPNKVMWSWSEAWEVYEQNGGALFKDLERY	313
DmpN	GIRPPKYVEQTTIGKEHITHQVWGALYQYSKATSFHTWIPGDEELNWLSEKYPDTFDKYY	374
α -subunit	GIRPPKYQDVANDAKHHLSHQLWTFYQYCQATNFHTWIPEKEEMDWMSEKYPDTFDKYY	373
DmpN	RPRFEFWREQQAKGERFYNDTLP HLCQVCQLPVI FTEPDDPTKLSLRSLVHEGERYQFCS	434
α -subunit	RPRYEYLAKEAAAGRFRFYNN TLPQLCQVCQIPTIFTEKDAPTMLSHRQIEHEGERYHFCS	433
DmpN	DGCCDIFKNEPVKYIQAWLPVHQIYQGNCEGGDVETVVQKYYHIKSGVDNLEYLGSPEHQ	494
α -subunit	DGCCDIFKHEPEKYIQAWLPVHQIYQGNCEGGDLETVVQKYYHINIGEDNFDYVVGSPDQK	493
DmpN	RWLALKGQTPPTAAPADKSLGAA	517
α -subunit	HWLSIKGRK-----PADKNQDAA	511

Figure 5. Sequence alignment of *Pseudomonas sp.* CF600 DmpN and *Pseudomonas sp.* OX1 PHH α -subunit. The Zn^{2+} binding site of both subunits is coordinated by four cysteine residues: C400, C402, C433 and C437 in DmpN and C399, C401, C432 and C436 in PHH α -subunit (shaded **C** indicates the cysteines involved in Zn^{2+} binding). The alignment was generated through NCBI Protein Blast program. Accession numbers: D37831 (DmpN) and 3U52_A (α -subunit). Similarity between the two sequences is 79% identity.

Although the crystal structure of phenol hydroxylase in *Pseudomonas sp.* CF600 is not available, we were able to use the hydroxylase of OX1 strain to compare sequences and determine the possible Zn^{2+} binding domain and its coordination with the four cysteine residues. The role of the Zn^{2+} binding site has yet to be determined in both DmpN of CF600 and in the α -subunit of OX1, though the hypothesis that it may be have a role in stabilization of the C-terminal domain the PHH subunit has been suggested³⁷.

Roles of Zn^{2+} in Enzymes

Zinc is the second-most abundant metal element found in nature, after iron, and it is required for biological functioning in living organisms. The earliest finding of a zinc-dependent metalloprotein was carbonic anhydrase, which is an enzyme that catalyzes the interconversion between carbon dioxide and bicarbonate³⁸. It was discovered by Keilin and Mann in 1939.³⁹ Since this discovery, more than 300 other zinc-containing proteins from six classes of enzymes have been identified.⁴⁰ Because zinc ions contain filled d-orbitals and are stable as Zn^{2+} , they do not participate in redox reactions, and instead serve as Lewis acids by acting as electron pair acceptors.⁴¹ Zn^{2+} found in proteins has been shown to play catalytic and/or structural roles.

Catalytic Roles of Zn^{2+} in Enzymes

For a wide range of enzymes, catalytic Zn^{2+} is found at the active site and is involved in the interaction with the substrates.⁴² Zn^{2+} can form 4, 5 and 6-coordinated complexes and have ligands that are labile, which are important properties for metals that behave as catalysts.⁴³ In general, in enzyme active sites Zn^{2+} coordinates to three amino acid side chains that can be a combination of histidine (H), glutamate (E), aspartate (D) and cysteine (C), along with a solvent molecule that completes a tetrahedral coordination sphere⁴² (reviewed in 16). In a review article⁴⁴ where 12 Zn^{2+} -containing enzymes were surveyed, it was determined that histidine is the most common ligand found in the active site followed by glutamate, aspartate and cysteine.

Catalytic Zn^{2+} in enzymes usually participates in the breaking and forming of bonds during conversion of substrate to product. In the case of carbonic anhydrase II, the active site Zn^{2+} is involved in activating a hydroxide ion for nucleophilic attack in the hydrolysis reaction⁴⁵. The catalytic site can also be involved in stabilizing ligands with a carboxylate and polarization

of carbonyl groups that are involved in reactions catalyzed by the enzyme, such as in human fibroblast collagenase⁴⁶. Zn^{2+} can also be involved in stabilization of charge in the transition state of a reaction⁴² (reviewed in 88).

Structural Role of Zn^{2+}

Zn^{2+} can have structural instead of catalytic roles in proteins. For example, Zn^{2+} stabilizes the quaternary structure of aspartate transcarbamylase, which catalyzes the conversion of L-aspartate and carbamoyl phosphate to carbamoyl-L-aspartate⁴⁷. As detailed in a review article⁴⁸, zinc fingers are another example where Zn^{2+} plays a role in the stabilization of protein structures, most notably DNA binding domains. In general, Zn^{2+} ligands are commonly located in flexible loops instead of a rigid secondary structure, and these interactions stabilize not only the local but also, the overall structure of the enzyme⁴². Formation of tetrahedral geometry coordinated by four amino acid side chains for catalytic ions has been reported, with the difference being that the solvent is not a ligand. Also, in the formation of a tetradenate complex with Zn^{2+} , cysteine side chains are the most common in structural Zn^{2+} centres because of the high affinity constants which stabilize the structure⁴⁹. In the oxygenase component of phenol hydroxylase, Zn^{2+} is bound by four cysteine residues, which hints that it participates in maintaining structural stability of the protein.

Zn^{2+} Chelators

Zn^{2+} binds tightly to proteins that contain it, and in order to perform studies on the binding site chelators are often used to first remove the metal ion. Many chelators have been shown capable of sequestering Zn^{2+} , including *N,N,N,N*-tetrakis (2-pyridylmethyl) ethylenediamine (TPEN) and ethylenediaminetetraacetic acid (EDTA) (Fig. 6). The dissociation

constants^{50,64} of these chelators to Zn^{2+} are $10^{-15.6}$ and $10^{-16.6}$ M, for TPEN and EDTA, respectively. These chelators are not only specific to Zn^{2+} , but can also be used for extraction of other metals, such as Fe^{2+} , with dissociation constants^{50,64} of $10^{-14.6}$ M for TPEN and $10^{-14.3}$ M for EDTA. Both chelating agents form hexadentate complexes, where TPEN sequesters metal ions through its six nitrogen atoms, and EDTA does so with the two nitrogen atoms and four carboxylic acid groups.

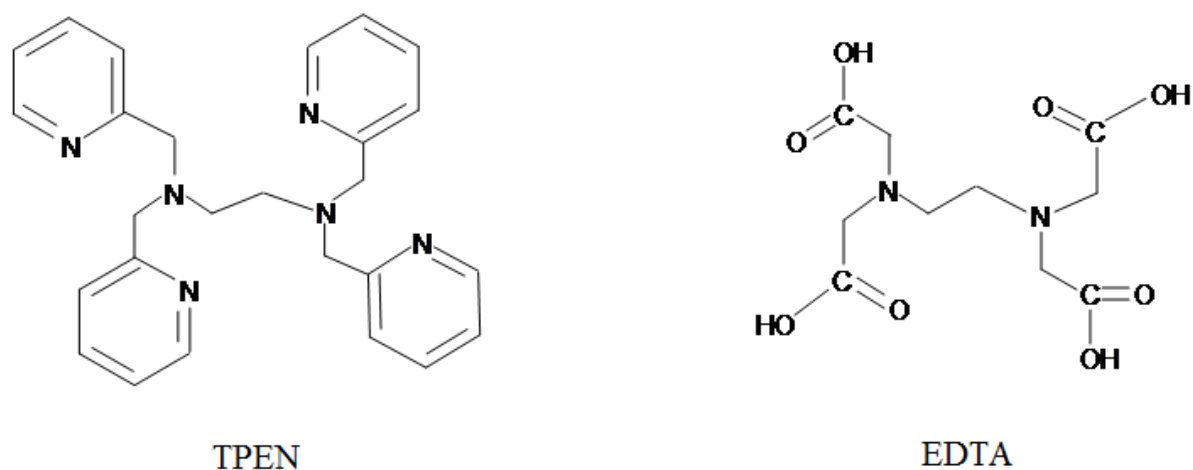


Figure 6. Structure of metal chelators used in this study. *N,N,N,N*-tetrakis (2-pyridylmethyl) ethylenediamine (TPEN) and ethylenediaminetetraacetic acid (EDTA).

YHS Domain

Pfam is a database with a collection of protein families that have been manually curated to catalogue the presence of domains and their functions in different proteins.^{51,52} Amino acid sequence alignments allow us to identify these conserved domain regions in proteins and may suggest roles that these domains play.⁵³

The YHS domain, as its name implies, is a short region of approximately 50 amino acids that has conserved tyrosine (Y), histidine (H) and serine (S) residues⁵². YHS domains that are

present in ATPases, such as those involved in copper transport, are thought to participate in metal binding since it is a heavy-metal transporter, although there is not enough evidence to support this hypothesis^{54,52}. It is interesting to note that a YHS domain is found in the larger subunit of oxygenases in multicomponent phenol hydroxylases that are also associated with DmpK-like proteins⁵⁴. In *Pseudomonas* sp. strain CF600, the Zn²⁺ binding site is found in the YHS region. As discussed above, DmpK is believed to be involved in facilitating association of apo-oxygenase with iron, and it has been shown to physically associate with the large oxygenase subunit. Together, these observations suggest that the YHS domain may play a role in the interaction between DmpK and the oxygenase, as well as assembling iron into the apo-oxygenase^{Error! Bookmark not defined.}.

Specific Objectives

Although extensive studies on the iron binding site of phenol hydroxylase in *Pseudomonas* sp. strain CF600 have been carried out^{33,34}, the Zn²⁺ binding site located in the large subunit of the oxygenase in this and other phenol hydroxylases has been minimally studied. The goal of this project was to study the role of Zn²⁺ in phenol hydroxylase structure and function. As is evident from the review presented above, by comparison with Zn²⁺ binding sites in other proteins, the tetradentate cysteine ligation suggests that a structural role is most likely for the Zn²⁺ in phenol hydroxylase.

Initially, the role of Zn²⁺ was experimentally approached by substituting one of the conserved cysteine ligands for Zn²⁺ in the oxygenase protein from *Pseudomonas* sp. strain CF600. It proved impossible to produce any variant oxygenase in soluble form, so the second approach was to devise a method to successfully remove Zn²⁺ from its binding site using

chelators, reducing agents and denaturants. Once the metal ion has been removed, it would enable further experiments to test how the structure and/or function of the oxygenase have changed.

MATERIALS AND METHODS

Materials

The LMW Calibration Kit Amersham™ For SDS Electrophoresis was from GE Healthcare (Baie d'Urfé, QC) and albumin standards for BCA assays were obtained from Fisher Scientific (Ottawa, ON). TPEN, NADH, ampicillin and carbenicillin were purchased from Sigma (Oakville, ON); EDTA, DTT and IPTG were from BioShop (Burlington, ON). DNaseI was purchased from Roche (Laval, QC) and Chelex®100 resins were obtained from BioRad (Mississauga, ON). Reagent A and Reagent B for Pierce BCA Protein assays were from Thermo Scientific (Ottawa, ON).

SDS-PAGE

Sodium dodecyl sulfate polyacrylamide gel electrophoresis (SDS-PAGE) was used to estimate the molecular weights of proteins, to estimate the purity of protein preparations, and to confirm the presence of a protein of interest. All protein samples were separated using a 12% acrylamide separating gel and 3.9% acrylamide stacking gel, as previously described⁵⁵, with some modifications. Briefly, samples were mixed with an equal volume of 2-fold concentrated reducing sample buffer, containing SDS, β -mercaptoethanol and bromophenol blue. Electrophoresis was conducted at 200V for 40 min using a BioRad minigel apparatus. A Coomassie staining solution (0.1% Coomassie Blue R-250, 40% methanol and 10% acetic acid) and destaining solution (10% methanol, 10% acetic acid and 2% glycerol) were used to enable the visualization of the protein bands on the gel. The molecular weight standards consisted of phosphorylase b (97 kDa), albumin (66 kDa), ovalbumin (45 kDa), carbonic anhydrase (30 kDa),

trypsin inhibitor (20.1 kDa) and α -lactalbumin (14.4 kDa) and were purchased as a mixture from GE Healthcare.

Protein Concentration Estimation

All phenol hydroxylase oxygenase (monomer) component (native and treated) concentrations were estimated using trichloroacetic acid (TCA) precipitation to remove interfering compounds, followed by the bicinchoninic acid (BCA) assay, essentially as described.⁵⁵ Briefly, samples were first incubated with 0.15% (w/v) sodium deoxycholate for 15 min at room temperature and then centrifuged at 16,060 x g with 3.2% (w/v) trichloroacetic acid for another 15 min before re-dissolving the pellet with 5% (w/v) SDS in 0.1% NaOH (25 μ L). Triplicates of each sample were prepared. Albumin standards were used and prepared at concentrations of: 0 mg/mL, 0.025 mg/mL, 0.125 mg/mL, 0.25 mg/mL, 0.5 mg/mL, 0.75 mg/mL, 1 mg/mL and 1.5 mg/mL before mixing with the working reagents. These concentrations of standards were used to generate the standard curve. The working reagents were prepared by mixing a 50:1 ratio of Reagent A: Reagent B. The assay mixture was incubated at 60 °C for 30 min on a heating block and allowed to cool on ice for 5 min before reading the absorbance at 562 nm with the Bio-TekPowerWave HT microplate reader.

Bacterial Growth and DmpLNO Expression

The expression of the DmpLNO oxygenase component of phenol hydroxylase was performed by transforming pPOW100 (*dmpK* inserted into the plasmid), as previously described.⁵⁶ Mutant plasmids of variant oxygenase encoding cysteine (C) to alanine (A) substitutions (C433A and C437A) were generated as previously described⁵⁷ and bacterial growth and expression were

performed at 37 °C (following wild-type protein procedure) or at 18 °C for 16 h or 48 h. The cells were grown in Luria Broth (LB) medium with 100 µg/mL ampicillin or carbenicillin antibiotic. After OD₆₀₀ reached between 0.8-1.0, a final concentration of 0.5 mM IPTG was added to cultures for induction at 37 °C for 3 h. Cells were collected by centrifugation at 14,295 x g with a JA-10 rotor, and cell paste was stored at -80 °C until further use.

Crude Extract Preparation for Purification of DmpLNO

The cell paste (20-25 g) was resuspended in a buffer of 50 mM Tris-HCl (pH 8.0) and 10% glycerol (2 mL buffer/gram of cell paste), and a few milligrams of DNaseI were added, as previously described.⁵⁸ Sonication of cells was performed at 10 bursts of 15 s on ice and a final concentration of 200 µM ferrous ammonium sulfate was then added from a stock solution in 10 mM HCl. Cell debris was removed using the Beckman Coulter Optima L-100 ultracentrifuge with Ti45 rotor at 104,350 x g for 1 h at 4 °C. The supernatant was used for the purification of DmpLNO as described below.

Purification of Phenol Hydroxylase DmpLNO

The purification of the oxygenase component, DmpLNO, was performed as previously described, at 4 °C with minor modifications. A brief description is given below.

Fast-Flow DEAE-Sepharose Column (2.6 x 22.7 cm). The anion-exchange column was washed with distilled water and equilibrated with 50 mM Tris-HCl (pH 8.0) containing 10% glycerol (“TG buffer”) before loading the crude extract. Unbound proteins were eluted with 75 mM NaCl in TG buffer. A gradient of 75-275 mM NaCl in TG buffer was applied at a flow rate of 6 mL/min to elute the oxygenase component. The OD₂₈₀ of the fractions was measured to estimate

protein concentration, while the detection of DmpLNO protein in the fractions was performed by SDS-PAGE, using a previously-purified DmpLNO sample for comparison. Fractions containing the oxygenase were pooled and brought to 65 % saturation with ammonium sulfate (40.4g $(\text{NH}_4)_2\text{SO}_4$ in 100 mL solution), and incubated at 4 °C for 30 min before collecting the precipitate after centrifugation at 15,303 x g for 30 min. The pellet was dissolved in a minimum volume of 30 mL TG buffer, and the solution was centrifuged at 3,826 x g for 20 min, and the supernatant was then loaded onto the next column. The Fast-Flow DEAE Sepharose column was washed and stored in 2 M NaCl.

Phenyl Sepharose High Performance Column (2.6 x 13.5 cm). The hydrophobic interaction column was washed with distilled water and equilibrated with TG buffer containing 0.15 M NaCl. Once the concentrated sample (30 mL) from the previous step was loaded, the same equilibration buffer was used for elution until the fractions were no longer visibly yellow in colour. TG buffer was then applied and the column was washed until the OD_{280} of the eluate dropped below 0.2 before eluting DmpLNO with 5 mM Tris-HCl (pH 8.0), containing 10% glycerol at a flow rate of 2 mL/min. The fractions with the highest OD_{280} absorbance values and eluted with DmpLNO (as judged SDS-PAGE analysis) were pooled together. The pooled fractions were brought to a 50 mM buffer concentration with 1 M Tris (pH 8.0), before concentrating to 5 mL using ultrafiltration with an Amicon YM30 membrane. The column was washed and stored in 50% ethylene glycol.

Sephacryl S-300HR Gel Filtration (2.6 x 77.2 cm). This size-exclusion column was equilibrated with TG buffer before loading the concentrated sample from the Phenyl Sepharose purification step. The oxygenase was eluted with the same buffer at a flow rate of 1 mL/min. Fractions

showing the higher OD₂₈₀ values and the highest purity of DmpLNO (as judged by SDS-PAGE analysis) were pooled and concentrated by ultrafiltration with an Amicon YM30 membrane. The column was washed and stored in 0.03% sodium azide in TG buffer.

Phenol Hydroxylase Activity Assay

The assay was performed at 25 °C in 1 mL of 50 mM Tris acetate (pH 7.5) buffer containing 345 μM NADH, 0.78 μM DmpP, 0.24 μM DmpM, 0.65 μM DmpLNO and catechol 2,3-dioxygenase as previously described³⁶. A final concentration of 1.23 mM phenol was added, initiating the two step reaction converting phenol to catechol and from catechol to the yellow-coloured product, 2-hydroxymuconic semialdehyde. The activity was monitored at OD₄₀₀ ($\epsilon_{400} = 18\ 800\ \text{M}^{-1}\ \text{cm}^{-1}$) using the Varian CARY 50 Bio UV Visible Spectrophotometer over a period of 1 min at 25 °C.

Apo-oxygenase Preparation

All glassware, microfuge tubes and pipette tips for this procedure were treated with 7-10% HNO₃ for at least 1 h and rinsed with ultrapure water before use, or allowed to dry in a 37 °C incubator overnight.

Dialysis Method. Native oxygenase (9 – 11 μM) was incubated with different combinations of DTT (2 mM), EDTA (5 mM), TCEP (2 mM), TPEN (5 mM), and urea (0.5 M) at room temperature or 4 °C over a period of at least 16 h. SpectraPor[®] Membrane with a MWCO 6-8K from Spectrum Laboratories Inc. (Rancho Dominguez, CA) was used for dialysis to remove metals, chelating, denaturing and/or reducing agents. The membrane was originally stored in EDTA (1 mM) and 25% ethanol solution and soaked in Chelex-treated TG buffer before use.

Samples were first dialysed against Chelex[®] 100-treated TG buffer at 4 °C. The buffer was changed a total of three times over a period of three days for all the samples.

NAP-5 Column Method. Samples were passed through a NAP-5 column for buffer exchange. The column was equilibrated with three bed-volumes of metal-free TG buffer. A volume of 0.4 mL sample was applied to the column followed by 0.1 mL metal-free TG buffer. Collection of the sample in a metal-free tube was done following the addition of 0.85 mL metal-free buffer.

Mini Chelex[®] Column Treatment. The proteins were first passed through the NAP-5 column (as above). The eluted sample was then transferred to a mini-Chelex[®] column (5 cm) and the eluate was collected.

Liquid Chromatography Inductively-Coupled Plasma Mass Spectrometry (LC-ICP-MS) Analysis⁵⁹

Native or apo-oxygenase proteins (2.2 – 4.5 µM) in a final volume of 200 µL were digested in 10% HNO₃ at 50 °C until the precipitate was solubilized (which could take up to a period of 5 days and a loss of 10-20 µL of sample had occurred). Digested proteins were diluted 10-fold in ultrapure water and submitted for LC-ICP-MS (Agilent 7500ce) analysis, along with a sample of ultrapure water, Chelex[®]100-treated TG buffer and the last dialysis buffers of each sample. External or internal standards were used for the calibration method. External standards used were Fe²⁺ and Zn²⁺ metals at concentrations of 1, 5, 10, 50 and 100 ppb (slight concentration changes may be applied for different sample preparations, but these values were mostly used). Internal standards were prepared by adding a 100 µL mixture of scandium and germanium metals to 1 mL of Fe²⁺ and Zn²⁺ standard solutions (prepared the same way as external standards) and samples.

Spectroscopic Analysis

Sample Preparation. A concentration of ~1 μM DmpLNO protein was used for CD and fluorometric analyses.

Circular Dichroism. Secondary structure changes and protein stability were analysed using far-UV CD spectroscopy. All CD spectra of samples were scanned at 25 $^{\circ}\text{C}$ using a Jasco-815 CD spectrometer. The spectra were collected over an average of 5 scans between the region of 200-260 nm using a 0.2 cm path length cell (containing ~400 μL of sample) with a scan rate of 20 nm/min and response time of 1 sec. The reported spectra resulted from a 0.2 nm data pitch, 1 nm bandwidth and sensitivity of 100 mdeg.

For thermal denaturation analysis, Jasco Pelletier temperature control was used with the same cell path length as above, and spectral changes were monitored at a wavelength of 222 nm, from 25 to 95 $^{\circ}\text{C}$ with a temperature slope of 25 $^{\circ}\text{C}/\text{h}$ and response time of 0.25 sec. A 0.2 $^{\circ}\text{C}$ data pitch, 2 s delay time, 1 nm bandwidth and 100 mdeg sensitivity were used to generate the spectra.

Fluorescence Spectroscopy. Tertiary structure changes and stability were probed using fluorescence spectroscopy. Fluorescence emission spectra were collected at 25 $^{\circ}\text{C}$ or between 25 and 80 $^{\circ}\text{C}$ or 95 $^{\circ}\text{C}$ at intervals of 5 $^{\circ}\text{C}$ using a Varian Cary Eclipse Fluorescence Spectrophotometer. Samples (~600 μL) were loaded into a 5 mm self-masking quartz cuvette (two sides with clear windows). The spectra were obtained between 300 and 400 nm, with excitation at 280 nm and slit widths of 5 nm. The voltage was set at MED with a fast scan speed collecting spectra over an average of 10 scans.

A Single Cell Pelletier temperature control unit was used in thermal denaturation analysis of the native protein between 25 and 95 °C at 5 °C intervals. Manual temperature control was used for denaturation of treated protein samples between 25 to 80 °C, at 5 °C intervals. The settings of the fluorometer were the same as above. The samples were equilibrated for 30 s after the temperature stabilized before taking a scan.

Generation of Fluorescence Intensity and Wavelength Graphs

The highest intensities at each temperature point were determined from the raw data of the fluorescence emission spectrum. The wavelength maximum that was estimated corresponds to the highest fluorescence intensity unit at the specific temperature.

Estimation of T_m values

T_m values were estimated by taking the average of the temperatures of the point where the curve begins to increase at the bottom of the sigmoidal curve and the point where it starts to level off at the top of the curve.

RESULTS

Wild-Type Oxygenase Purification from *Pseudomonas* sp. CF600

Purification of the wild-type oxygenase following the procedures outlined in *Materials and Methods* showed that the three subunits of the enzyme co-purify in all purification steps, as expected from previous results³⁵. The total amount of protein obtained from 25 g of cell paste was 72 mg (10.3 mg/mL), with a specific activity of 370 nmol/min/mg.

Variant Oxygenase Protein C433A & C437A Expression at 18 °C and 37 °C

Plasmids encoding phenol hydroxylase variants C433A and C437A were constructed by a former M.Sc. student, Amy Wong and retested for expression⁵⁷. Cell growth and expression of the protein in *E. coli* was performed as described in *Materials and Methods*. Inclusion bodies were obtained after growth either at 37 °C for 3 h or 18 °C for 16 h, (data not shown), which was also as observed previously⁵⁷.

Variant Oxygenase Protein C436A Expressed at 18 °C with Addition of Zn²⁺

The possibility that soluble protein yield could be improved by the addition of Zn²⁺ to the culture medium was tested using variant oxygenase C436A. The hypothesis is that the variant protein is destabilized by the loss of Zn²⁺, and higher concentrations of Zn²⁺ might allow the metal to bind and stabilize the structure. Bacterial growth conditions were the same as for native protein (*Materials and Methods*), but induction with IPTG was at 18°C for a period of 48 h rather than 16 h. A control uninduced sample was also prepared to compare with the results of expression under inducing conditions.

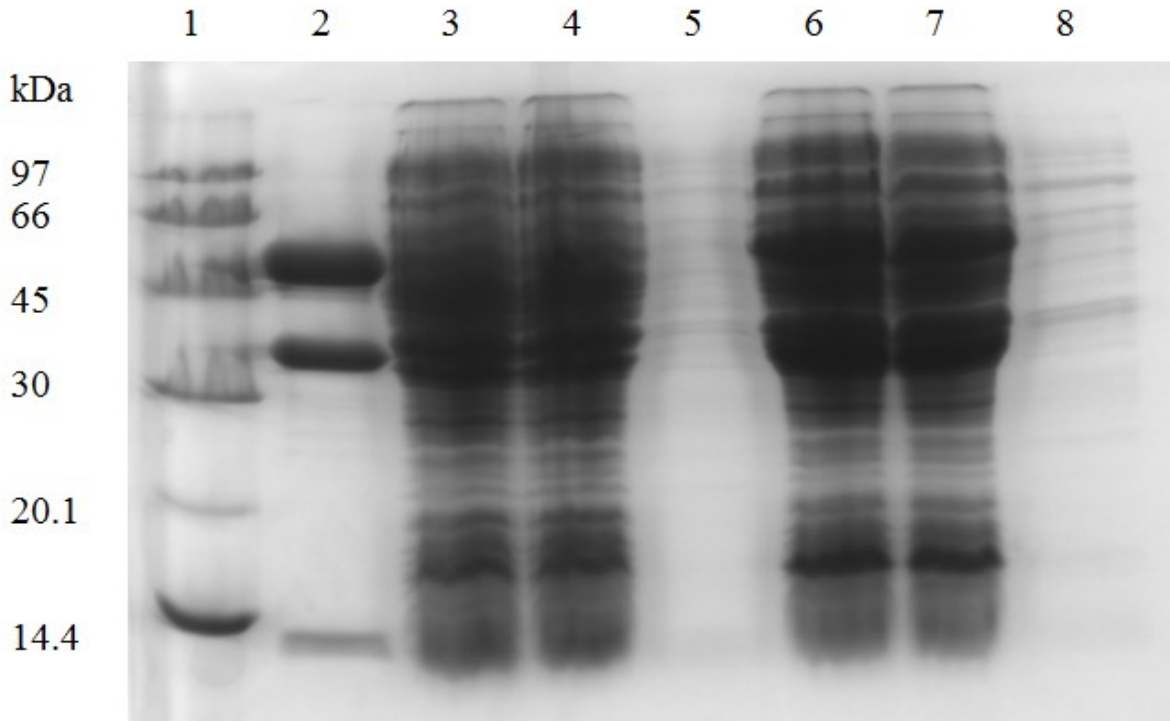


Figure 7. SDS-PAGE (12%) gel electrophoresis of C436A variant protein expressed at 18 °C for 48 h under inducing (with IPTG) and non-inducing conditions. Lane 1: low molecular marker; Lane 2: purified wild-type oxygenase; Lane 3: uninduced pellet; Lane 4: uninduced pellet after addition of Zn^{2+} ; Lane 5: uninduced supernatant after addition of Zn^{2+} ; Lane 6: induced pellet; Lane 7: induced pellet after addition of Zn^{2+} ; Lane 8: induced supernatant after addition of Zn^{2+} . All samples were diluted 1:1 with 2-fold sample buffer. 15 μ L of samples were loaded onto gel except the low molecular weight marker with a volume of 5 μ L.

After expression under inducing or non-inducing conditions at 18 °C for 48 h, the cell paste was resuspended in TG buffer (~1 g/mL), sonicated, and then centrifuged at 16,060 x g. The pellet was then resuspended in sample buffer and loaded onto the gel (Fig. 7 lanes 3 & 6). Increased DmpN expression was observed under inducing conditions as opposed to uninduced, although it was difficult to visualize if there was expression for DmpL and DmpO. These sonicated pellets were then resuspended in buffer containing added $ZnCl_2$ (2 mM) in an attempt to solubilize the protein, and then centrifuged to collect the supernatant, but most of the protein

still remained as inclusion bodies as there is very little protein found in the supernatant (lanes 5 & 8).

It is possible that the substitution of alanine for cysteine destabilizes the structure more than a cysteine to serine substitution. For that reason, expression of cysteine to serine variants in *E. coli* has also been attempted in our lab for each of the four cysteine residues (C400, C403, C433 and C437) that coordinate Zn^{2+} in the oxygenase. These proteins were expressed at 37 °C for about 3 h, or at 18 °C for at least 12 h, but under all conditions there was little expression of DmpN, DmpL and DmpO, and/or they were insoluble. (Dr. Elisabeth Cadieux, personal communication).

Alternative Strategy to Characterize the Zn^{2+} Binding Site

The difficulty in obtaining soluble protein after substituting the cysteine residues with alanine or serine residues prompted an alternative approach involving attempted removal of Zn^{2+} from the native enzyme. Considering the effects on the oxygenase structure of substituting any of the Zn^{2+} binding ligands, leading these variants to be found in inclusion bodies, it was anticipated that probes of structure such as fluorescence or circular dichroism spectroscopies might be useful in detecting changes at the Zn^{2+} binding site.

Chemical reagents such as chelators having high affinity for Zn^{2+} , reducing agents that could help prevent the formation of disulfide bonds between the four cysteine ligands, and denaturants to unfold the protein and aid in easier accessibility to chelators and reductants, were used in different combinations to attempt Zn^{2+} removal. Once Zn^{2+} has been removed, the effects

on enzyme structure and function can be examined by studying the apoenzyme and reconstituted holozyme.

Structure Stability of the Native Oxygenase Probed Using Circular Dichroism and Fluorescence Spectroscopies

Before attempting to remove Zn^{2+} , the native structure of the protein was first probed spectroscopically to set a baseline for comparison for metal ion removal experiments. Secondary and tertiary structures of the native oxygenase were examined using far-UV circular dichroism (CD) and fluorescence spectroscopies, respectively.

CD spectroscopy was used to probe the temperature stability of the native enzyme (Fig. 8). Fig. 8A shows the CD spectra of the native protein at 25 °C and 95 °C, and Fig. 8B is the thermal denaturation curve of the protein, as monitored by CD spectroscopy. Scans collected at 25 °C and 95 °C were corrected with the blank (TG buffer).

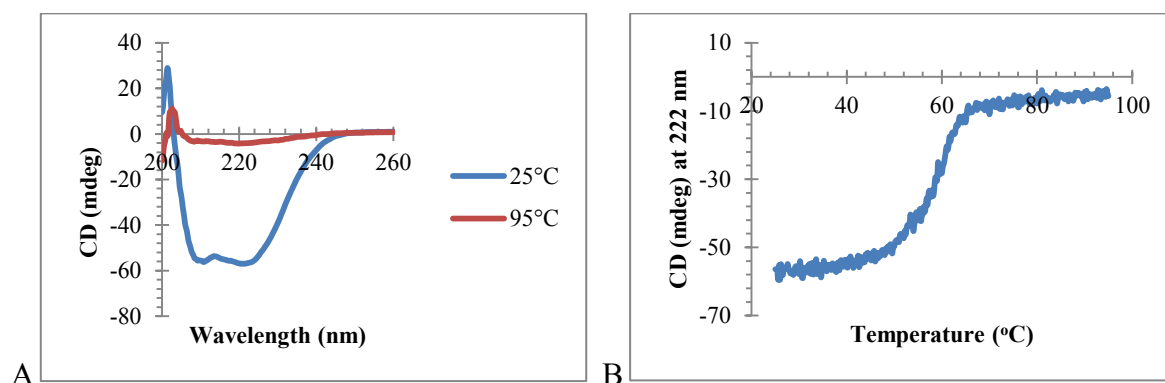


Figure 8. Circular dichroism studies of native oxygenase. A. Spectra at 25 °C and 95 °C. B. Thermal denaturation scan (25 to 95 °C) of native protein at a rate of 25 °C/h and wavelength of 222 nm. Final concentration of protein is 0.90 μ M.

The spectrum of the native protein at room temperature exhibits a double minimum at 222 and 208 nm characteristic of α -helical structure. At 95 °C, the α -helical structure is lost,

indicating protein unfolding and/or precipitation. As shown in Fig. 8B, with increasing temperature the ellipticity starts to decrease at around 45 °C and continues to decrease until 65 °C. An additional small change in signal then occurs from 65 to 95 °C. Insoluble protein was detected in the cuvette when it was removed from the CD spectrometer indicating irreversible denaturation. Intrinsic fluorescence was used to monitor the effects of temperature on the tertiary structure of the native protein. Fig. 9A shows the intrinsic fluorescence emission spectra of oxygenase, upon excitation at 280 nm, as a function of increasing temperature.

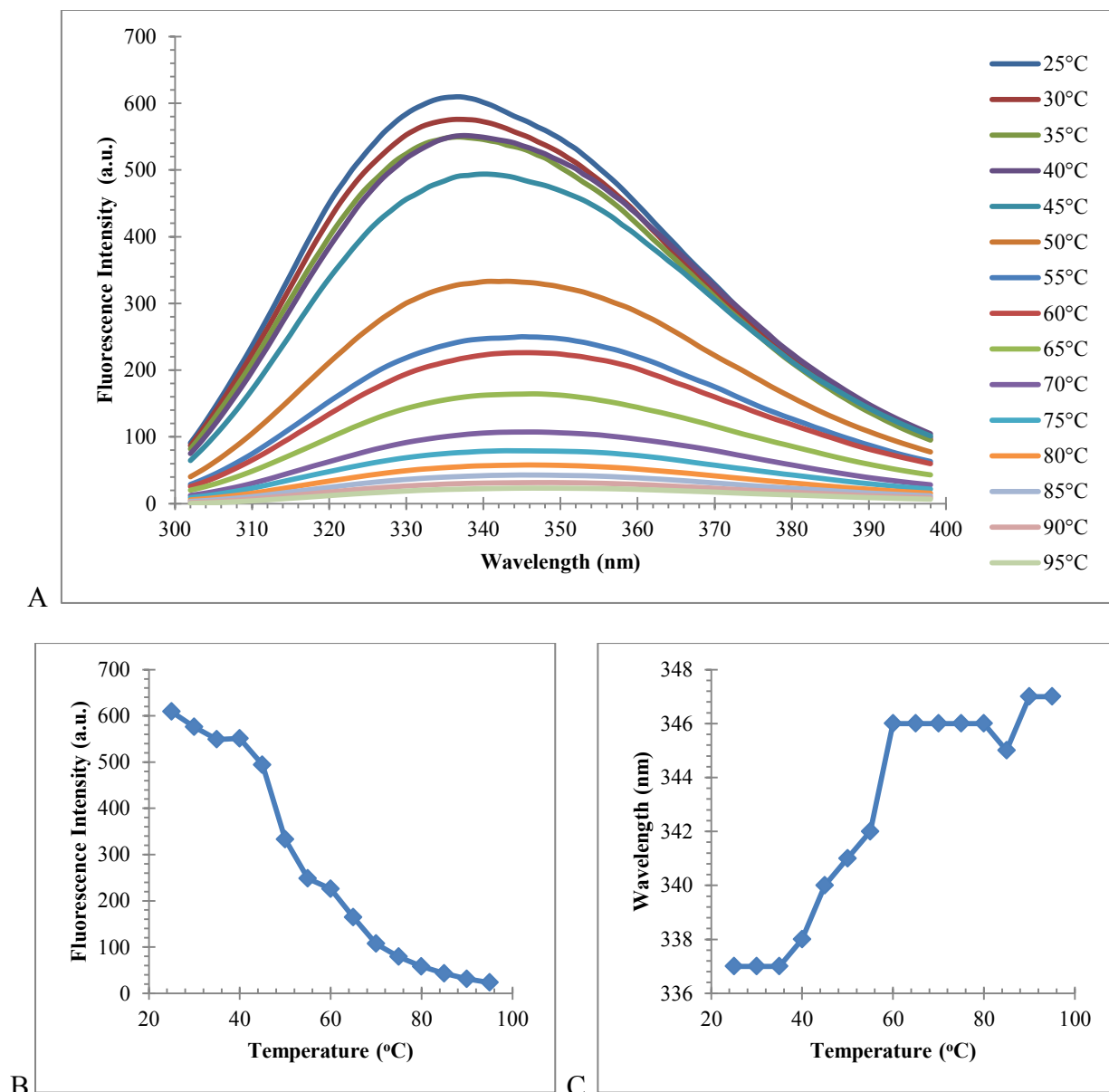


Figure 9. Intrinsic fluorescence spectra of native oxygenase as a function of temperature. A. Fluorescence spectra at temperatures from 25 to 95 °C. B. Change in fluorescence intensity with temperature. C. Red-shift of emission wavelength maximum with increasing temperature. Excitation wavelength in all experiments was 280 nm. Concentration of sample was 0.90 μ M.

The temperature range where the largest change in emission intensity takes place is from 45 to 60 °C (Fig. 9B), which is very similar to the temperature dependence of the CD signal (Fig.

8B). A spectral red-shift occurred as the temperature increased, consistent with the exposure of buried aromatic amino acids (tyrosine and tryptophan) to a more polar environment as the protein unfolded. The red-shift appeared to cease when the sample reached 60 °C, the same temperature at which ellipticity change ceased (Fig. 8B). The decrease in fluorescence intensity that accompanies the red shift was also observed with the increase in temperature, which results in the lowering of the quantum yield as a consequence of the tryptophan residues⁶⁰ being exposed to the polar solvent⁶¹ as well as the higher temperature.

Metal Content in Native Oxygenase

To examine the metal content of the native oxygenase protein, ICP-MS was used. Seven different samples were prepared for ICP-MS analysis using three different preparations of purified oxygenase. Samples were digested with 10% HNO₃ and diluted 11-fold with ultrapure water for analysis, as described in “*Materials and Methods*”. Table 1 below shows the results of iron and zinc content measurements for different samples of native oxygenase.

Number of metal ions per dimer of native oxygenase protein		Metal Species	
	Sample Number	Fe ²⁺	Zn ²⁺
	1	4.6	2.9
	2	3.4	3.1
	3	3.4	2.3
	4	3.9	3.0
	5	4.3	3.1
	6	4.5	3.1
	7	N/A	2.0
	Standard Deviation	0.5	0.5
Average	4.0	2.5	

Table 1. ICP-MS metal analysis of iron and zinc in native oxygenase protein. The average of iron and zinc content was calculated using the results of the 7 sample preparations. Final concentration of samples varied between 0.45 to 5 μ M. N/A represents not applicable data.

Iron content was measured on each of six different preparations (average of triplicate or quadruplicate data of each preparation) of oxygenase, whereas zinc content was measured seven times, and the final average of all measurements was taken. Previously, the iron and zinc content using ICP-MS of native DmpLNO expressed with DmpK purified from *E. coli* (without addition of ferrous ammonium sulphate during isolation) showed that each monomer of oxygenase had 1.4 Fe and 0.7 Zn, which corresponds to 2.8 Fe and 1.4 Zn in the dimers³⁵. The iron content obtained from the expression of DmpLNO in the presence of DmpK (with ferrous ammonium sulphate) in *Pseudomonas* sp. CF600 were between 2.4 to 3.6 mol Fe²⁺ per mol of oxygenase³⁴. In the phenol hydroxylase oxygenase component of *Pseudomonas* sp. OX1, an orthologous protein of *Pseudomonas* sp. CF600 oxygenase, iron and zinc content were four and two mol per

mol of oxygenase, respectively^{Error! Bookmark not defined.}. We obtained $4.0 \pm 0.5 \text{ Fe}^{2+}/\text{mol}$ oxygenase and $2.5 \pm 0.5 \text{ Zn}^{2+}/\text{mol}$ oxygenase, which agree quite well with the values obtained previously.

Overview of the Zn^{2+} -Chelating Experiments

In order to remove Zn^{2+} from the enzyme, treatments with various combinations of chelators (EDTA, TPEN), reductants (DTT, TCEP) and mild denaturants (low concentrations of urea) in conjunction with dialysis were attempted. Another method that was used was chromatography on Chelex, a metal ion-binding resin.

Metal Analysis of DTT-Treated Oxygenase

The Zn^{2+} at the binding site is believed to be coordinated by four cysteine residues (C400, C403, C433 and C437) through thiol- Zn^{2+} bonds. It is thus possible that the presence of the reductant could stimulate the removal of Zn^{2+} . Its presence may also help keep the cysteine residues reduced if Zn^{2+} is removed through dialysis. Thus, incubation of the oxygenase with DTT (2 mM) over a period of 16 h at room temperature was followed by dialysis of samples against Chelexed-TG buffer lacking DTT, with two buffer changes over a two day period, at 4 °C. Samples were then digested with 10% HNO_3 and diluted 11-fold before ICP-MS analysis. Table 2 below shows the metal content for DTT-treated protein before and after dialysis.

Samples	Metal Species	Mol metal ions per mol protein
DTT before dialysis	Fe ²⁺	3.4
	Zn ²⁺	2.5
DTT dialysed	Fe ²⁺	3.0
	Zn ²⁺	2.6*

* This value was the average of 4 values with a standard error of 0.3

Table 2. ICP-MS analysis of iron and zinc in DTT-treated oxygenase before and after dialysis. Final concentrations of the samples were 2.7 μ M.

Iron and zinc contents were examined and compared to untreated protein (Table 1) to determine whether either of the metals was removed during treatment with DTT/dialysis. As is shown in Table 2, iron and zinc contents were essentially the same before and after dialysis. This indicates that DTT alone was not sufficient to facilitate Zn²⁺ release from the enzyme.

Spectroscopic Analysis of Oxygenase Treated with EDTA and DTT

To assist in extraction of Zn²⁺ from the enzyme, an effective chelator, ethylenediaminetetraacetic acid (EDTA), was introduced into the sample in addition to the reducing agent, DTT⁶². Oxygenase was incubated with either EDTA (5 mM) alone, or EDTA (5 mM) and DTT (2 mM), overnight at room temperature, followed by dialysis the next day at 4 °C against metal-free buffer containing EDTA only, or EDTA/DTT. This was followed by two rounds of dialysis against metal-free buffer without EDTA or DTT.

The far-UV CD spectra of the EDTA/DTT-treated proteins before dialysis (Fig. 10A) show that at 95 °C, the α -helical structure is lost as compared to the 25 °C scan: this behaviour is essentially the same as for native oxygenase (Fig. 8). However, when the oxygenase was treated

with EDTA and DTT, then dialyzed, the CD spectrum at 95 °C indicates that the α -helical structure is not completely lost (Fig. 10B). The thermal denaturation curves of the four EDTA or EDTA/DTT-treated samples confirm that complete denaturation is achieved with samples before dialysis, but after dialysis, the samples do not completely denature (Fig. 10C).

The transition midpoint temperatures, T_m , (determined by taking the average temperature between the lowest and highest CD signal) of the denaturation curves for pre-dialysis EDTA and EDTA/DTT treated samples were 57 °C, which is similar to T_m for the native protein of 54 °C. After dialysis, the T_m values for EDTA and EDTA/DTT treated samples were shifted 5 to 7 °C (to 52 °C and 50 °C, respectively). Thus, in addition to incomplete denaturation after EDTA treatment and dialysis, the stability of the oxygenase appears to be lower.

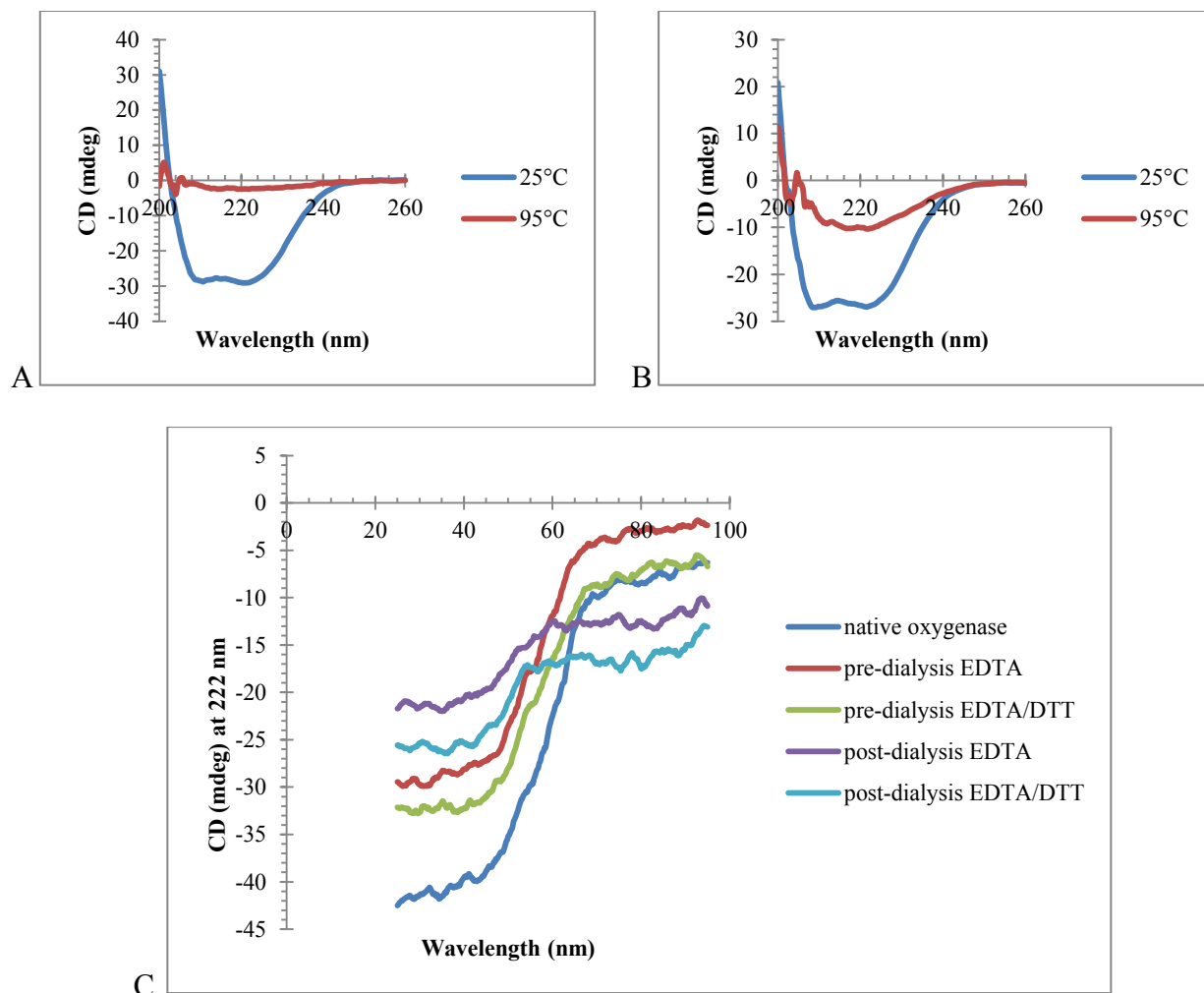


Figure 10. Far-UV CD spectra of EDTA and EDTA/DTT treated samples pre- and post-dialysis. A. EDTA and DTT-treated oxygenase (before dialysis) scans at 25 °C and 95 °C. B. EDTA and DTT-treated oxygenase (after dialysis) scans at 25 °C and 95 °C. C. Thermal denaturation curves of native oxygenase (control) and treated oxygenase pre- and post-dialysis at a wavelength of 222 nm with a scan rate of 20 nm/min. Final protein concentrations were 0.90 μM . Note: Spectra after treatment of oxygenase with EDTA alone are not shown, but they have the same spectra as samples treated with EDTA/DTT.

Temperature denaturation of these samples was also monitored by fluorescence spectroscopy (Fig. 11). In these experiments, it was only possible to monitor changes up to 80 °C, which is the limit of the thermostatted water bath. For each sample, the wavelength maximum at 25 °C was between 335 to 338 nm, and the wavelength maximum shifted in a similar fashion as the temperature increased to 80 °C: however, the peak maximum of the

dialysed samples shifted to somewhat higher wavelengths compared to those samples that were not dialyzed (Fig. 11B). The fluorescence signal intensity decreased with increasing temperature in a similar fashion for all samples (Fig. 11A).

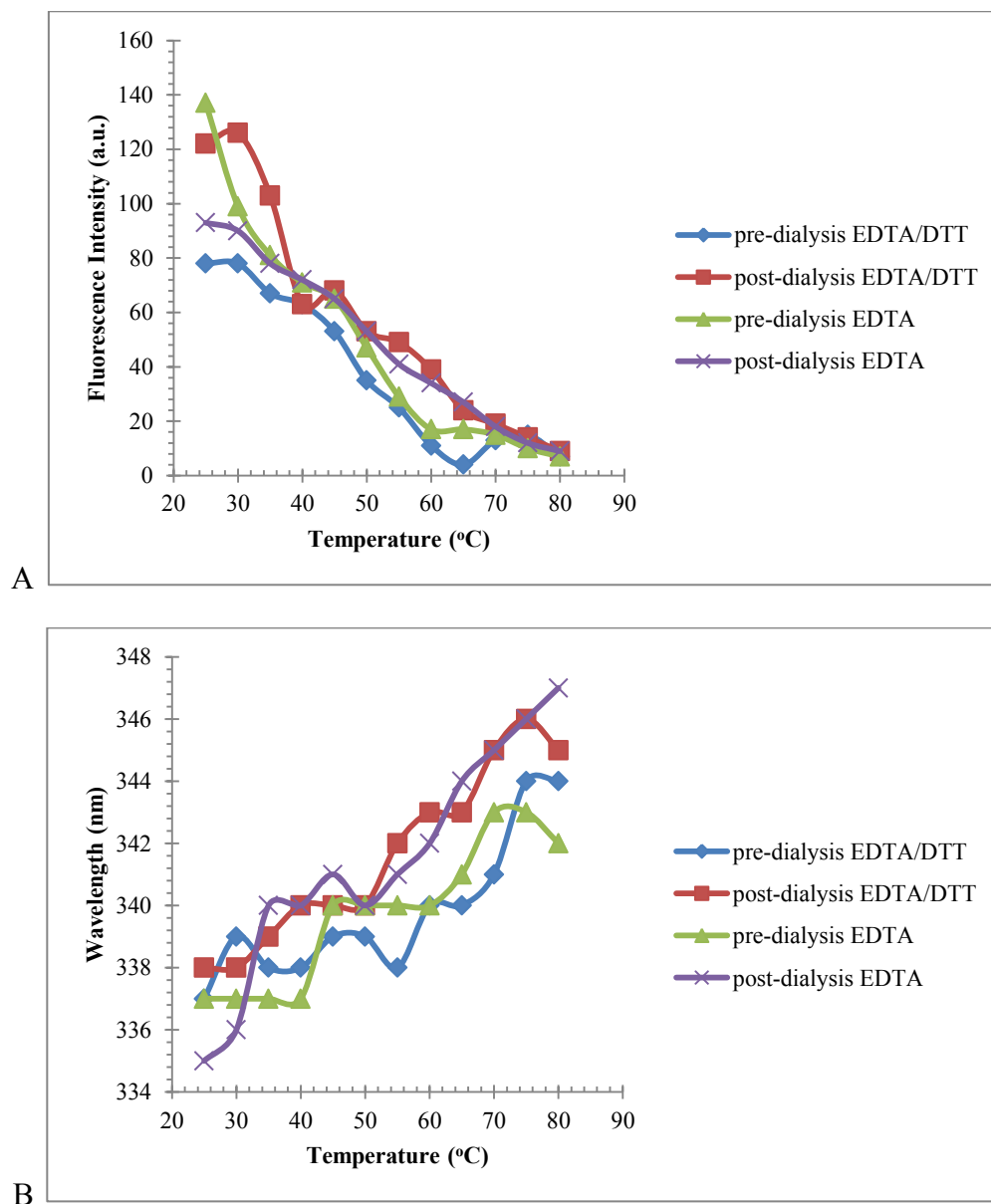


Figure 11. Intrinsic fluorescence of EDTA and EDTA/DTT-treated oxygenase pre- and post-dialysis as a function of temperature. A. Fluorescence intensity changes with increasing temperature. B. Peak emission wavelength changes with increasing temperature. Excitation wavelengths in all experiments were performed at 280 nm. Scans were collected at every 5 °C from 25 to 80 °C. The samples were from the same preparations used for far-UV CD scans (Fig. 10).

Metal Analysis of EDTA-Treated Samples

Iron and zinc contents for dialysed and incubated samples (from the same stock used previously for CD and fluorescence analysis) are shown in Table 3. These data indicate that the EDTA or EDTA/DTT treatments, with or without dialysis, were unable to eliminate iron or zinc from the oxygenase despite the fact that the stability of the protein is affected by the different treatments, as is evident from preceding spectroscopic analysis.

Samples	Metal Species	Mol metal ions per mol protein
EDTA pre-dialysis	Fe ²⁺	4.4
	Zn ²⁺	3.0
EDTA post-dialysis	Fe ²⁺	5.7
	Zn ²⁺	2.9
EDTA/DTT pre-dialysis	Fe ²⁺	4.7*
	Zn ²⁺	3.3*
EDTA/DTT post-dialysis	Fe ²⁺	3.4*
	Zn ²⁺	2.7*

*These values were the average of two values that differed at most by 10%

Table 3. ICP-MS metal analysis of iron and zinc in oxygenase protein samples. Final concentrations of samples were 2.2 to 2.7 μ M.

Spectroscopic Analysis of TCEP-Treated Oxygenase in the Presence and Absence of EDTA

A reducing agent that is more stable and more effective than DTT in preventing formation of disulfide bonds is Tris(2-carboxyethyl)phosphine (TCEP)⁶³. This reductant was tested as an alternative to DTT: samples were incubated with EDTA (5 mM) and TCEP (2 mM) overnight (~ 16 h) and then dialysed against Chelex[®]-treated TG buffer that contained EDTA and TCEP in the first round of dialysis overnight at 4 °C. The next two changes of buffer did not include the chelator and reducing agent. Fig. 12 shows the CD spectra at 25 °C and 95 °C as well

as the thermal denaturation curves for the two oxygenase samples that were incubated overnight with TCEP or TCEP/EDTA, pre- and post-dialysis. .

The T_m values for TCEP and TCEP/EDTA treated oxygenase (prior to dialysis) were approximately 56 °C, which is essentially the same as for the EDTA and EDTA/DTT treated samples (Fig. 10A & B). After dialysing the two treated samples, T_m values dropped to 50 °C for TCEP-treated oxygenase and 51 °C for the TCEP/EDTA-treated sample, consistent with those observed after EDTA/DTT treatment.

Figs. 12A & B show the spectra at 25 °C and 95 °C of samples of post-dialysis TCEP/EDTA-treated and TCEP-treated oxygenase, respectively. At 25 °C, both spectra show the α -helical character of the protein, but after denaturation at 95 °C, the α -helicity is lost. This can be better observed in the CD thermal denaturation scan (Fig. 12C) where both pre-dialysis TCEP and TCEP/EDTA treated samples denature completely after 65 °C, as indicated by the decrease in ellipticity to almost 0 mdeg. The CD signal for dialysed proteins, however, starts to level off at -35 mdeg at 55 °C and does not change much after that.

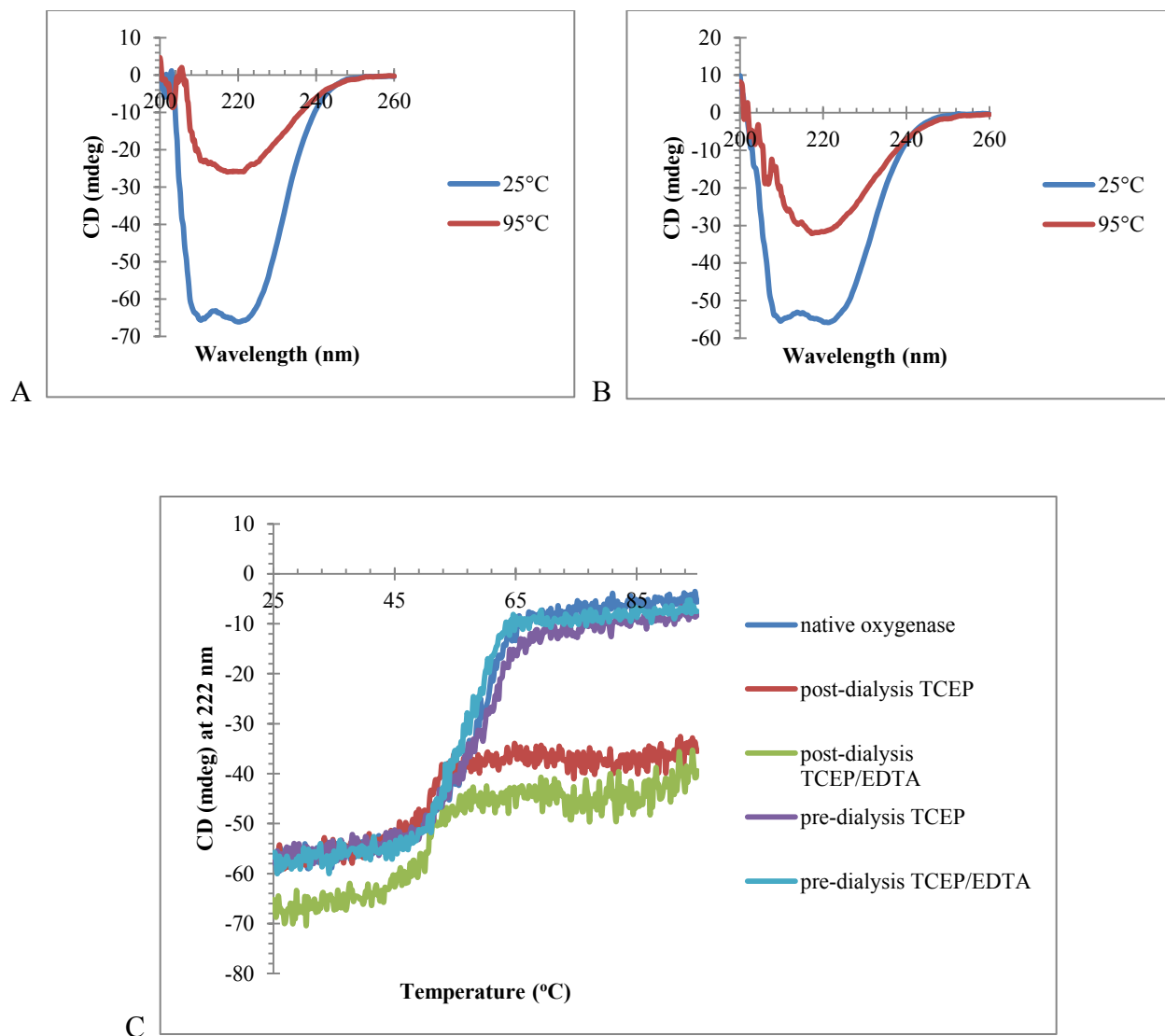


Figure 12. CD spectra and thermal denaturation curves of pre- and post-dialysis TCEP and TCEP/EDTA-treated oxygenase samples. A. CD spectra of TCEP (2 mM) and EDTA (5 mM)-treated oxygenase, after dialysis, at 25 °C and 95 °C. B. CD spectra of TCEP (2 mM)-treated oxygenase after dialysis at 25 °C and 95 °C. C. CD thermal denaturation curves of TCEP-treated oxygenase in the presence or absence of EDTA. Scans were performed at room temperature, and thermal denaturation scans were taken between 25 to 95 °C at a rate of 25 °C/h. Final concentration of protein was 0.90 μ M.

Thermal denaturation of these samples was also examined using fluorescence spectroscopy as a probe. The decrease in fluorescence intensity (Fig. 13A) and shift in wavelength of the emission maximum as a function of temperature are shown. The reduction in

fluorescence intensity commences immediately after 40 °C and continues to drop steadily until the end of the temperature scan at 95 °C. The shift in emission maximum wavelength starts at 40 °C and appears to stabilize when the temperature reaches 65 to 70 °C. None of the dialysed samples heated to 95 °C showed visible precipitates as compared to the samples before dialysis, where protein precipitate was observed after heating.

The change in wavelength of the maximal signal in the fluorescence spectra of all four samples seems to have stabilized at 55 °C (Fig. 13B), which is similar to the T_m values (51 to 56 °C) of the treated samples determined from the denaturation spectra (Fig. 12C), but the fluorescence intensity of the samples still continues to decrease with increasing temperature (Fig. 13A).

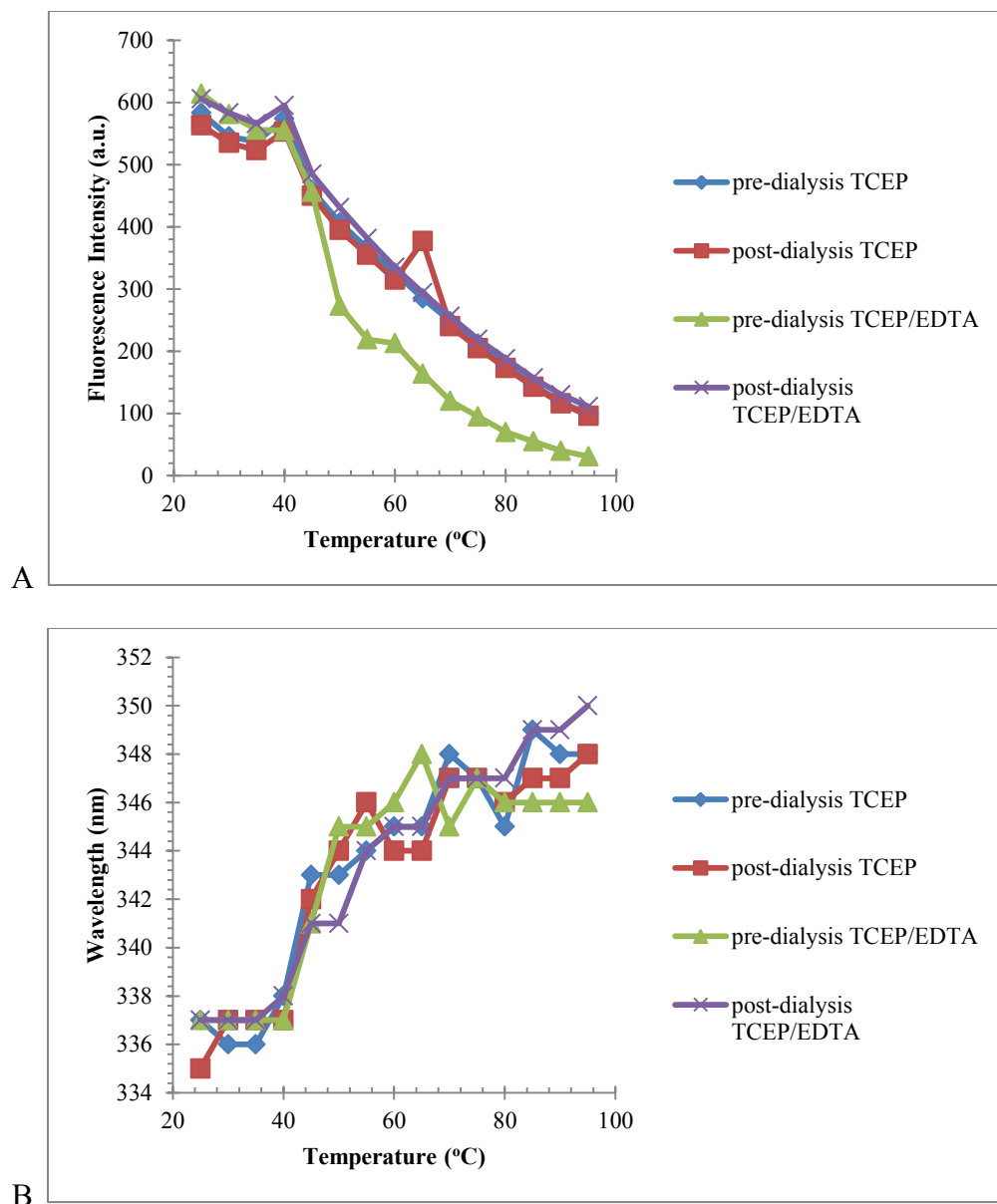


Figure 13. Intrinsic fluorescence intensity of TCEP- and TCEP/EDTA treated oxygenase samples pre- and post-dialysis. A. Fluorescence intensity change with increasing temperature. B. Emission wavelength maximum changes with increasing temperature. Excitation wavelength for all samples was at 280 nm. Spectra were collected at every 5 °C from 25 to 95 °C. The values in the graphs were generated from the recorded spectra (not shown). The samples were from the same preparation used for far-UV CD analysis.

Metal Content in Oxygenase after TCEP Treatment

The results from the temperature denaturation experiments monitored by CD and fluorescence spectroscopies indicate that there are structural differences between TCEP-treated samples before and after dialysis. ICP-MS on the two dialysed TCEP- and TCEP/EDTA-treated samples show that there is no significant difference between all the treated samples compared to the native protein therefore, these results cannot be explained by loss of metal ions (Table 4).

Samples	Metal Species	Mol metal ions per mol protein
TCEP dialysed	Fe ²⁺	3.3
	Zn ²⁺	2.4
TCEP EDTA dialysed	Fe ²⁺	3.7
	Zn ²⁺	2.5

Table 4. ICP-MS metal analysis of iron and zinc in TCEP- and TCEP/EDTA-treated oxygenase pre- and post-dialysis. Samples were incubated at room temperature 16 h overnight before dialysis. Final concentrations of samples were 1.8 to 2.2 μ M.

Effects of Urea on the CD Spectra of Native Oxygenase

Since EDTA and thiol reagent treatment failed to remove metal ions from the oxygenase, additional reagents were tested for removal of Zn²⁺. In this section, the effects of the protein denaturant, urea, on the structure of the protein were examined. Varying concentrations of urea (0.5 to 6 M) were incubated with wild-type oxygenase at room temperature for 16 h, before analysis by far UV-CD spectroscopy. Fig. 14 shows the CD spectra of oxygenase after treatment with urea.

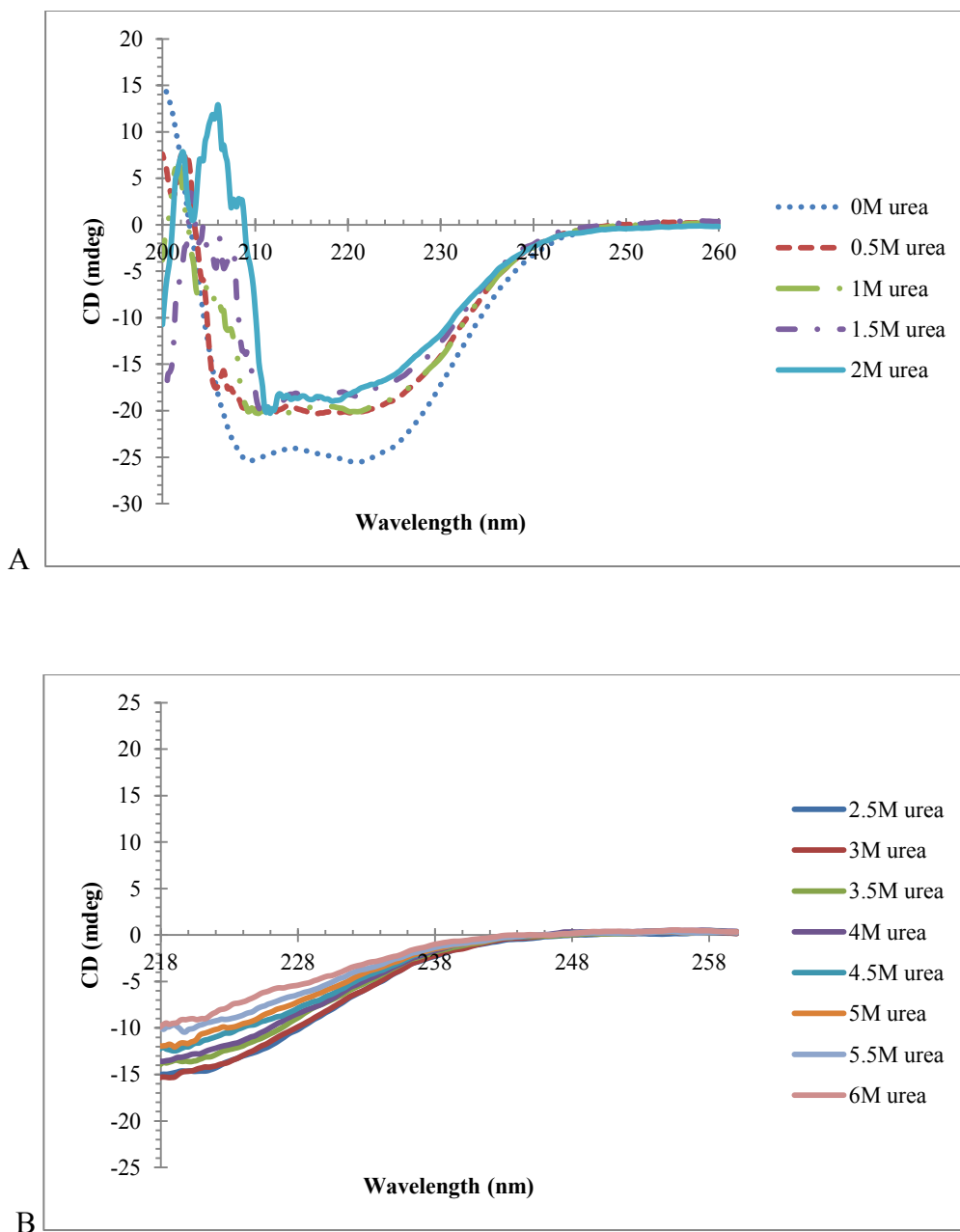


Figure 14. Circular dichroism spectra of native oxygenase incubated with varying concentrations of urea. Incubation of samples was at room temperature for 16h. A. Urea concentrations from 0 to 2 M. B. Urea concentrations from 2.5 to 6 M. Wavelength signals below 218 nm were cut off due to excessive noise. Samples (400 μ L) with 0.45 μ M protein at different urea concentrations were contained in a 0.2 cm path length cell. Each sample scan was the result of an average of five accumulations at room temperature with a scan rate of 20 nm/min.

Incubation of the oxygenase with 0 to 2 M urea showed an initial change in α -helical structure from 0 to 0.5 M, with very little additional change from 0.5 to 2 M (Fig. 14A). Experiments with 2.5 to 6 M urea are shown in Fig. 14B, and the steady decrease in CD signal indicates unfolding. The nature of the structural change that occurs with 0.5 M urea is not known, but it appears to perturb the structure without unfolding it.

Metal Content of Urea-Treated Oxygenase in the Presence of EDTA and DTT

Although results shown in the previous sections indicates that EDTA and DTT are ineffective in removal of metal ions from the oxygenase, the structural change caused by addition of urea (Fig. 14) may make it easier for reducing and chelating agents to gain access to the metal-binding site.

Initially, a concentration of 5 M urea was used to test whether denaturation by urea would facilitate the chelation of the metal ions. Oxygenase was incubated with EDTA (5 mM), DTT (2 mM) and urea (5 M) at room temperature for 6 h before dialysis at 4 °C. Initially, the metal-free dialysis buffer contained EDTA (5 mM) and DTT (2 mM), and subsequent buffer exchange was against only metal-free buffer. Dialysis buffers were changed three times over 3 days. As is shown in Table 5, after treatment with urea (5 M) and EDTA/DTT, followed by dialysis, almost all of the iron and zinc in the oxygenase were depleted. This result is expected since the protein appears to be mostly unfolded when in 5 M urea (Fig. 14B).

Samples	Metal Species	Mol metal ions per mol protein
pre-dialysis EDTA/DTT/urea	Fe ²⁺	N/A
	Zn ²⁺	1.9
post-dialysis EDTA/DTT/urea	Fe ²⁺	0.1
	Zn ²⁺	0.1

Table 5. ICP-MS metal analysis of EDTA/DTT and urea-treated oxygenase before and after dialysis. Oxygenase (60 μ M) was incubated with EDTA (5 mM), DTT (2 mM) and urea (5 M) at room temperature for 6 h before dialysis or stored. The final concentration of protein was 2.2 μ M. N/A represents not applicable data.

Metal Analysis of EDTA- and EDTA/DTT-Treated Oxygenase after Column Buffer Exchange

In this section, buffer exchange using a desalting column was tested as an alternative to dialysis. It is possible that prolonged dialysis risks introducing metal contaminants into apo-enzyme preparations and that this could be avoided by a more rapid desalting procedure. Oxygenase was treated with EDTA or EDTA/DTT at room temperature for 16 h, as in the previous experiments. Metal ions and reagents were removed through metal-free buffer exchange in a NAP-5 column, which takes a period of a few minutes compared to days with dialysis. Table 6 shows the number of metal ions that remained bound to the protein after treatment with chelator or absence of reducing agent.

Samples	Metal Species	Mol metal ions per mol protein
EDTA	Fe ²⁺	2.9
	Zn ²⁺	2.3
EDTA DTT	Fe ²⁺	2.4*
	Zn ²⁺	2.2*

* These values were the average of 2 values that differed by at most 30%

Table 6. ICP-MS metal analysis of EDTA- and EDTA/DTT-treated oxygenase after NAP-5 column purification. EDTA (2 mM) and DTT (5 mM) were incubated with oxygenase (11 μ M) at room temperature for 16 h before loading onto a mini-NAP-5 column. Final concentrations of samples were 0.2 to 0.5 μ M.

The Zn²⁺ content of both preparations was approximately two Zn²⁺ ions per mole of protein, indicating this method is ineffective in the removal of Zn²⁺. The iron content, however, was reduced to 2.9/mol protein without DTT addition and to 2.4/mol protein when DTT was added, as compared to 4.0/mol protein in the native enzyme (Table 1).

Temperature Denaturation of Samples Prepared Using the NAP-5 Column

The far-UV CD spectra of EDTA and EDTA/DTT-treated oxygenase samples desalted using NAP-5 columns (Figs. 15A & B) were similar to those observed for samples desalted using dialysis (Figs. 10A & B). After thermally denaturing the proteins by heating to 95 °C, the structures lost α -helicity but there was no obvious protein precipitate in the cuvette. As the temperature denaturation curves in Fig. 15C show, complete unfolding of the treated oxygenase samples were not achieved (unlike the wild-type sample), and the ellipticity at 222 nm for these samples remains around -15 mdeg. The T_m values for both EDTA-only and EDTA/DTT-treated oxygenase samples shifted to significantly lower temperature than the native enzyme (Fig. 15C), as was observed for dialysed samples from the earlier experiments.

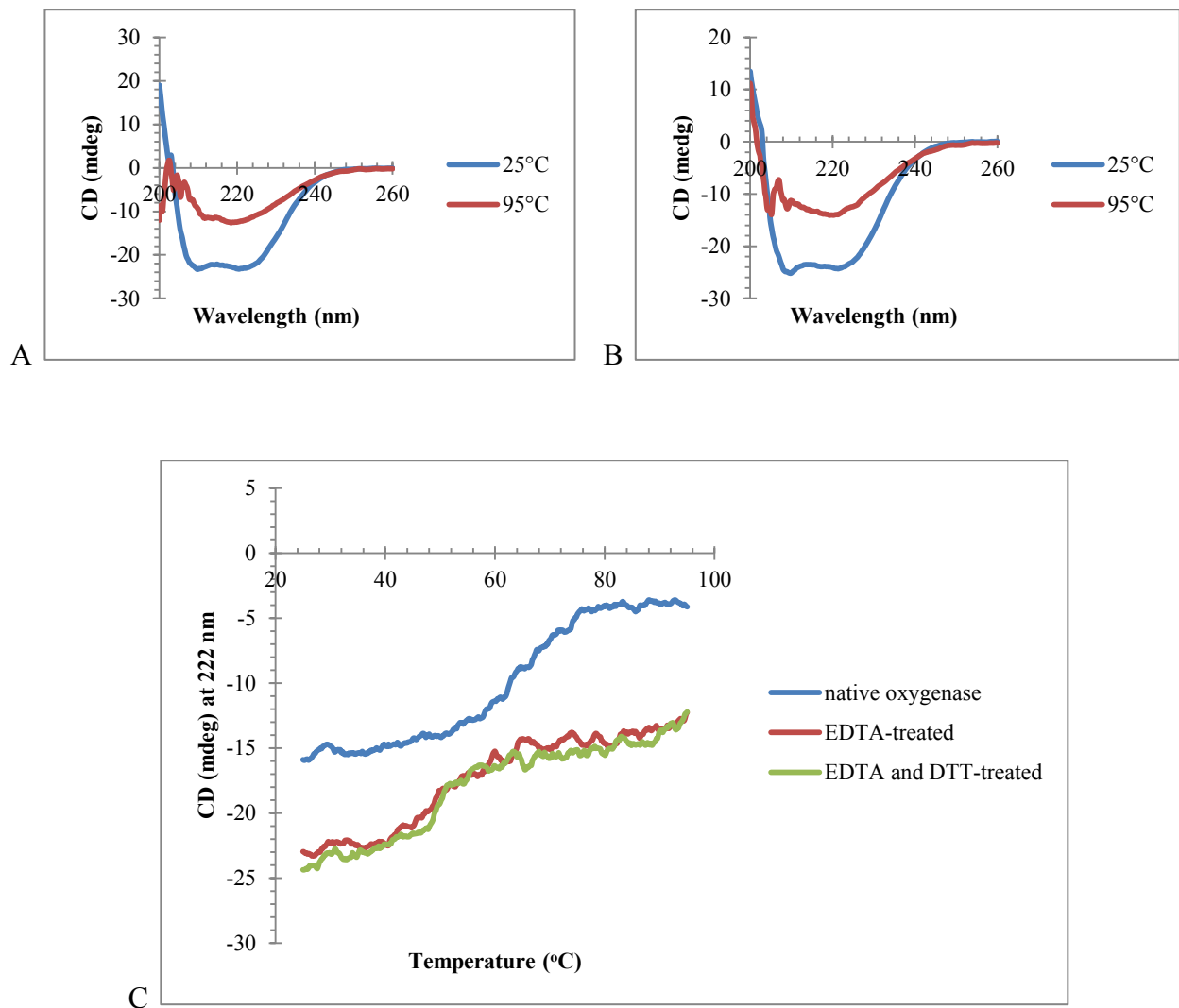


Figure 15. Far-UV CD spectra of EDTA-treated and EDTA/DTT-treated oxygenase after metal-free buffer column exchange with NAP-5. A. EDTA-treated oxygenase scans at 25 °C and 95 °C. B. EDTA/DTT-treated oxygenase scans at 25 °C and 95 °C. C. Thermal denaturation curves of native oxygenase (control), EDTA-treated and EDTA/DTT-treated oxygenase. All final protein concentrations were 0.45 μ M.

Temperature denaturation as followed by fluorescence spectroscopy for these treated samples that were desalted by NAP-5 chromatography (Fig. 16A & B) showed the same trend in

emission wavelength maximum shift and fluorescence signal decrease as the treatment with dialysis for EDTA and EDTA/DTT (Fig. 11A & B).

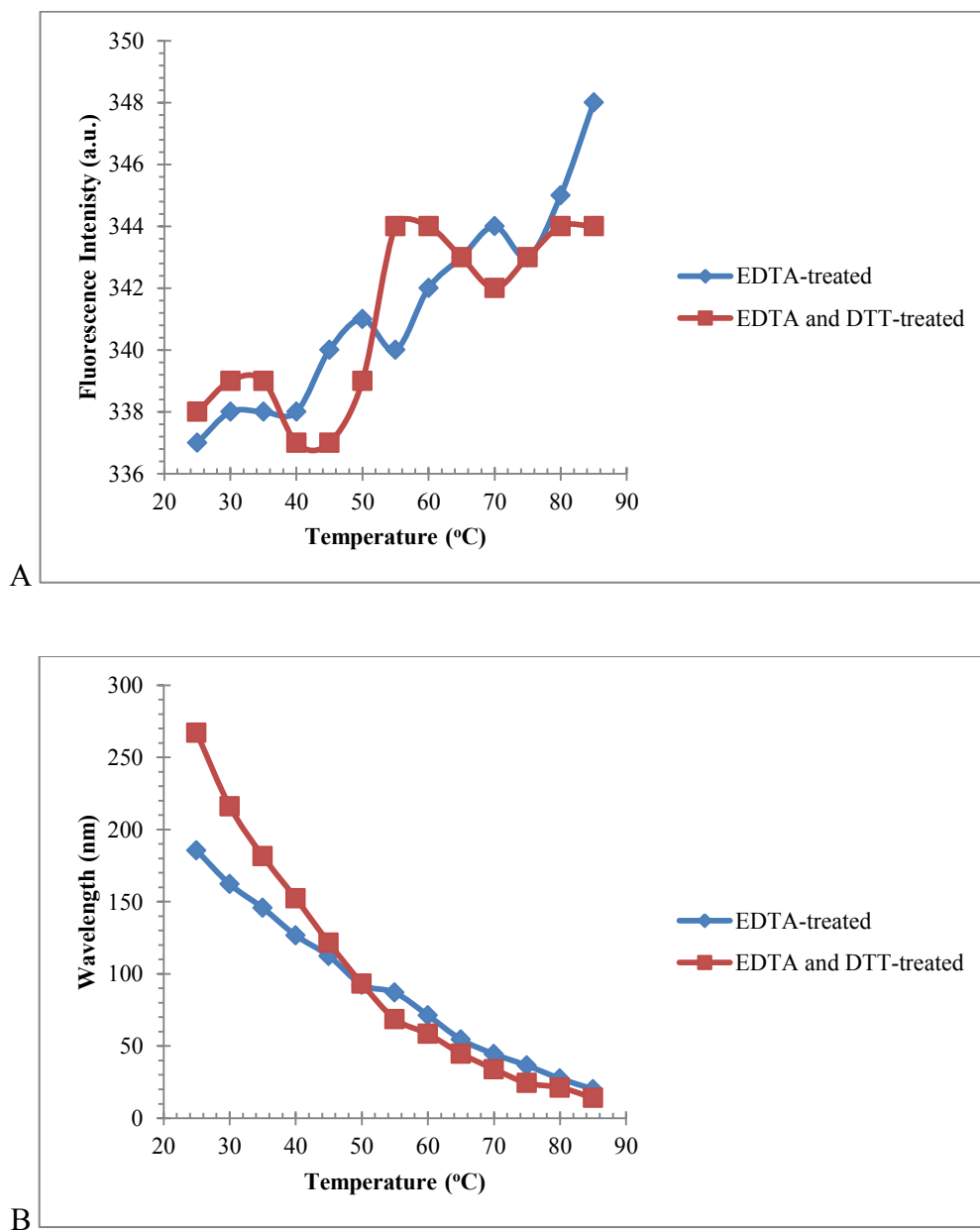


Figure 16. Intrinsic fluorescence monitored denaturation of EDTA and EDTA/DTT-treated-oxygenase desalted using a NAP-5 metal-free buffer exchange column. A. Fluorescence intensity changes with increasing temperature. B. Emission maximum wavelength changes with increasing temperature. All wavelength values were obtained from the highest fluorescence intensity units at the specified temperature. Scans were collected at 5 °C intervals from 25 to 80 °C. The samples were from the same preparation for far-UV CD analysis.

Metal Analysis of TPEN-Treated Oxygenase in the Presence of a Combination of DTT and/or Urea

The possibility that a metal ion chelator other than EDTA might be more effective at removal of Zn^{2+} was also tested. TPEN (*N,N,N',N'*-Tetrakis(2-pyridylmethyl)ethylenediamine) is a chelator that is known to have a high affinity for Zn^{2+} , and is permeable to cells⁶⁴. The oxygenase was incubated overnight with TPEN and DTT⁶⁵, with or without urea (0.5 M), before buffer exchange by dialysis. Metal-free buffer without TPEN and DTT was used for dialysis, and changed three times over a period of three days.

Prior to dialysis, all samples, both with and without urea, exhibited iron and zinc contents similar to the native oxygenase. After dialysis, however, both metal ion contents decreased as shown in Table 7. These results also show that urea (0.5 M) aided the removal of Zn^{2+} under these conditions. The structural changes induced by this low concentration of urea thus appear to aid the action of reducing and chelating agents in metal ion removal.

Samples	Metal Species	Mol metal ions per mol protein
pre-dialysis TPEN/DTT	Fe ²⁺	4.3
	Zn ²⁺	3.0
post-dialysis TPEN/DTT	Fe ²⁺	0.1
	Zn ²⁺	1.3
pre-dialysis TPEN/DTT/urea	Fe ²⁺	3.8
	Zn ²⁺	2.6
post-dialysis TPEN/DTT/urea	Fe ²⁺	0.3
	Zn ²⁺	0.1

All values were from the average of two values that differed by at most 20%

Table 7. ICP-MS metal analysis of TPEN and DTT-treated oxygenase in the presence or absence of urea, before and after dialysis. TPEN (5 mM), DTT (2 mM) and urea (0.5 M) were incubated with oxygenase (14.5 μ M) at room temperature 16 h before dialysis or storage. The final concentration of samples was 0.5 μ M.

Temperature Denaturation of TPEN-Treated Oxygenase

The temperature denaturation of TPEN/DTT/urea-treated oxygenase was monitored by far-UV CD spectroscopy (Fig. 17): samples pre- (Fig. 17A) and post-dialysis (Fig. 17B) are shown. At 95 °C, a limited CD signal is detected for either sample, and precipitate formed in the cuvette, indicating complete denaturation of the protein structure. Temperature denaturation curves in Fig. 17C show that ellipticity values at 222 nm at 25 °C for the native and treated proteins differ by 25 mdeg. This is consistent with Fig. 14A, where urea (0.5 M) induced a structural change that decreased the intensity of the CD signal in the 201 to 240 nm range, although apparently not to as great an extent.

The T_m value of the pre-dialysis TPEN/DTT/urea-treated sample (red line, 58 °C) is lower than the T_m of the post-dialysis sample (green line, 62 °C), although this may simply be due to the presence of urea in the pre-dialysis sample. Comparing these T_m values to that of the

native enzyme (blue line, 57 °C), treatment of the sample prior to dialysis is the same as the control and previous pre-dialysis samples (56 to 57 °C, Figs. 8B, 10C & 12C), but the dialysed TPEN/DTT/urea-treated sample gave a higher T_m value compared to other post-dialysis samples (range between 49 to 52 °C, Figs. 10C & 12C).

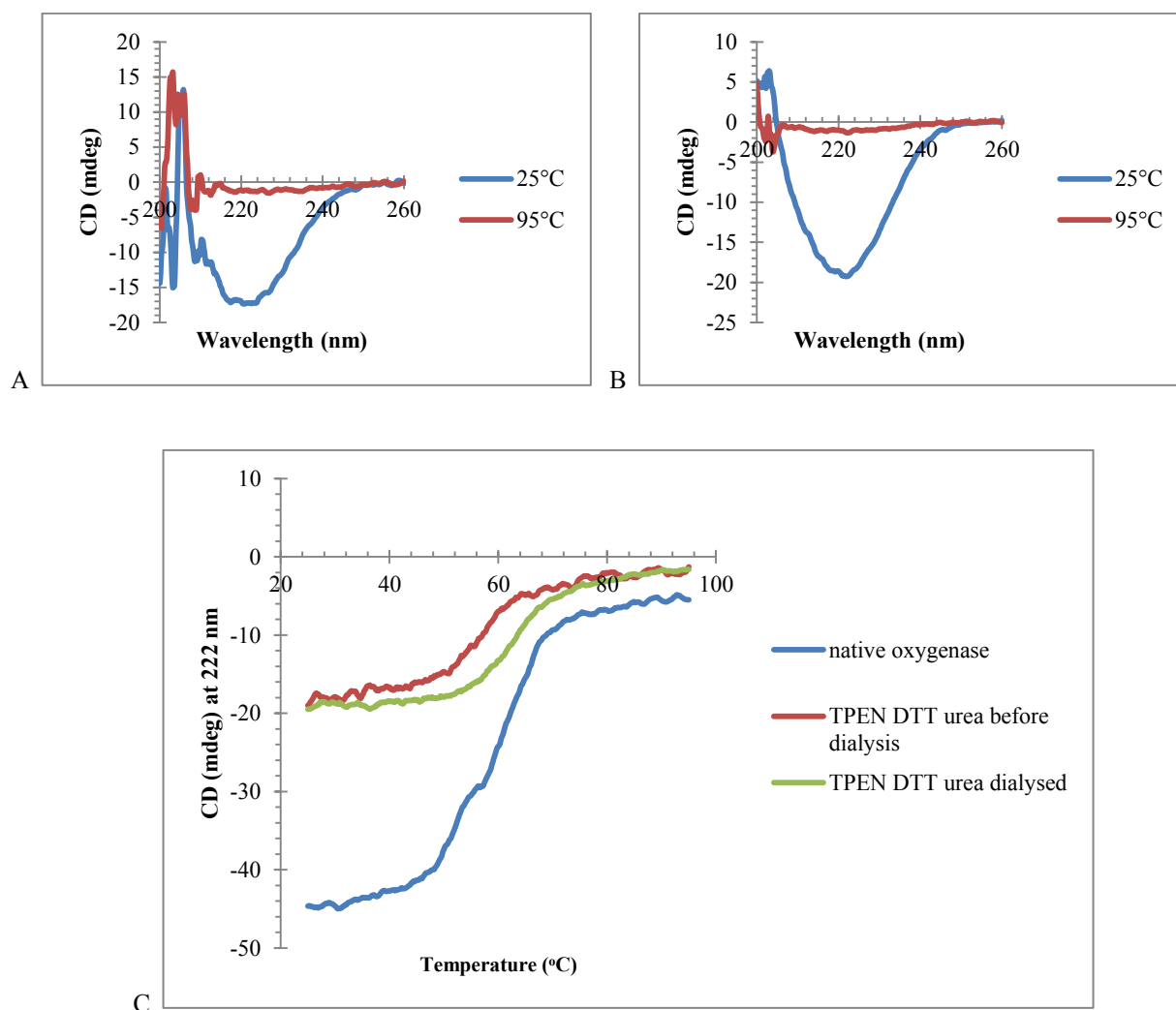


Figure 17. Far-UV CD spectra of TPEN/DTT/urea-treated oxygenase before and after dialysis. A. Variable temperature spectra (25 °C & 95 °C) of pre-dialysis oxygenase before dialysis. B. Treated post-dialysis oxygenase spectra at 25 °C and 95 °C. C. Thermal denaturation curves of native oxygenase (control) and treated oxygenase before and after dialysis. All final protein concentrations were 0.90 μM.

Temperature-induced denaturation was followed by fluorescence emission spectroscopy upon excitation at 280 nm (Fig. 18). The differences in starting fluorescence indicate structural differences between the samples that were dialyzed, compared to the undialyzed sample. At 80°C, the protein is unfolded as indicated by the very low fluorescence intensity signal and increase in wavelength. Only very small differences in response to temperature were noted in the emission wavelength maximum for the two samples (data not shown).

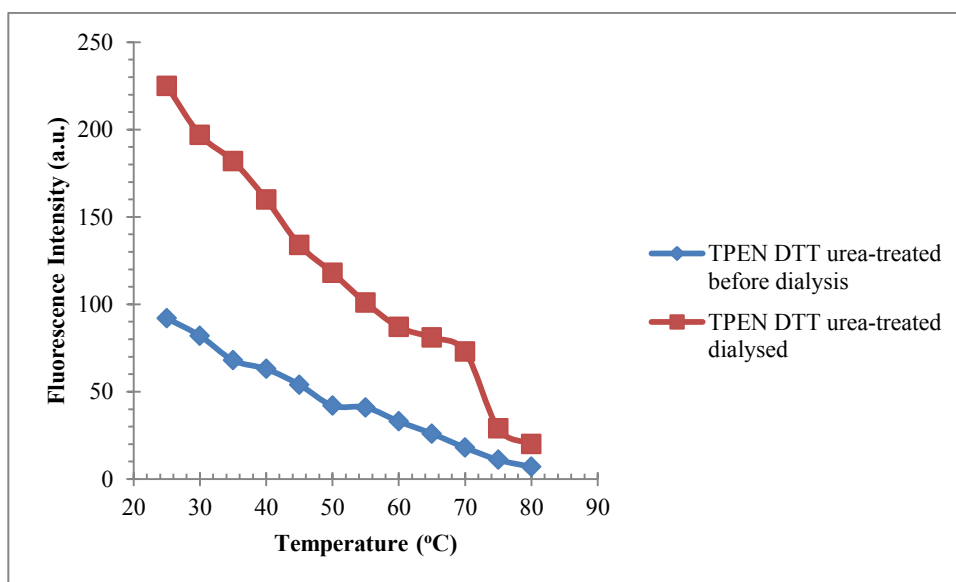


Figure 18. Intrinsic fluorescence to monitor denaturation of TPEN/DTT/urea-treated oxygenase, pre- and post-dialysis. Scans were collected at every 5 °C time points from 25 to 80 °C at an excitation wavelength of 280 nm. The samples were from the same preparation for far-UV CD analysis.

Metal Analysis of Oxygenase after Mini-Chelex[®] Purification

Another column method that was used to remove reducing, chelating, and denaturing reagents and metal ions was through an in-house generated mini-Chelex[®] column. The Chelex[®] resins are the same ones used to prepare the metal-free buffer, hence, the first step after

incubation with the appropriate reagents (refer to Table 8) was to buffer-exchange the samples with metal-free TG buffer in a NAP-5 column, then pass it through the mini-Chelex[®] column.

Samples	Metal Species	Mol metal ions per mol protein
DTT	Fe ²⁺	0.4
	Zn ²⁺	1.3
TPEN/DTT	Fe ²⁺	0.1
	Zn ²⁺	0.1
DTT/urea	Fe ²⁺	1.3
	Zn ²⁺	1.3
EDTA/DTT/urea	Fe ²⁺	1.4
	Zn ²⁺	1.1

Table 8. ICP-MS metal analysis of DTT-treated oxygenase in the presence or absence of EDTA, TPEN and urea after Chelex[®] treatment. DTT (2 mM) and TPEN (5 mM) samples without urea with oxygenase (14.5 μM) were incubated at room temperature for 16 h before treatment. DTT (50 mM), EDTA (5 mM) and urea (5 M) were incubated with oxygenase (14.5 μM) at room temperature for 6 h before treatment. Final concentrations of samples were 0.5 to 2 μM.

The results presented in Table 8 indicate that the combination of reagents that is the most effective at removing the zinc ion is TPEN with DTT, consistent with the previous TPEN-treated experiment (Table 7), decreasing the amount of zinc metal to 0.1/mol oxygenase. However, this also removed iron from the protein.

DISCUSSION

Phenol hydroxylase of *Pseudomonas* sp. CF600 is a multicomponent enzyme comprised of different subunits, with oxygenase (DmpLNO) being the component where hydroxylation occurs. The enzyme also has been isolated from other bacterial species, where it has a similar role. At the oxygenase active site, diiron centre metal ions are bound and coordinated by glutamate and histidine residues³⁷. The average number of iron atoms important for oxygenase activity³⁵ in the oxygenase is approximately 4, and zinc is also always found in metal analysis experiments³⁵.**Error! Bookmark not defined.**

The objective of this project was to determine the role of Zn^{2+} found in the oxygenase component of phenol hydroxylase. First, expression of variant oxygenases modified at one of the four cysteine residues was attempted, and when that failed, methods for generating an apo- Zn^{2+} enzyme were examined. No previous experimental studies have been reported on the Zn^{2+} binding site of this or similar oxygenases.

As was pointed out in the *Introduction*, two of the four cysteine residues that coordinate the metal ion binding site are found in the region of DmpN containing the YHS domain. This domain also includes a conserved tyrosine, histidine and serine-containing region that is found in all phenol hydroxylase enzymes that have a component similar to DmpK, previously shown to be important for the assembly of the active site into the oxygenase component, DmpLNO⁵⁴. The location of the YHS domain, residues 409-452 in the oxygenase⁶⁶, is important because it coincides with that of the Zn^{2+} binding site. The YHS domain may be involved in the assembly of the oxygenase component, since genes encoding DmpK-related proteins are encoded together with phenol hydroxylase genes that include a YHS region⁵⁴.

Variant proteins with a cysteine to alanine substitution at the zinc-binding site were previously prepared by a M.Sc. student in the lab, Amy Wong⁵⁷. There are four cysteine residues that coordinate the zinc-binding site (C399, C402, C432 and C436) in the α -subunit of *Pseudomonas* sp. OX1, as was shown in the structure determined by Sazinky *et al*³⁷. These amino acids in *Pseudomonas* sp. CF600 correspond to C400, C403, C433 and C437, respectively, of DmpN. Substitution of one or more of these cysteine residues, and characterization of the resulting variant enzyme, would provide information about the importance of Zn^{2+} , for example, about whether it plays a structural or catalytic role in the oxygenase.

Attempts to express and purify the variant proteins were originally performed by Amy Wong⁵⁷, using the same methods of expression and purification as for the wild-type oxygenase. Soluble protein expression was low, even at lower temperatures (18 °C), and the oxygenase subunits were mostly present in inclusion bodies. Attempts to purify the soluble enzyme suggested that the three subunits, DmpLNO, of all the variant oxygenase did not co-purify as in the native protein. This could be an indication that without the four cysteine coordination to keep Zn^{2+} in place, the protein's quaternary structure was destabilized, possibly helping to explain its presence in inclusion bodies.

In this study, an attempt was made to increase expression of soluble C437A variant oxygenase. A small modification in the procedure included increasing the period for protein expression to 48 h from 16 h. In addition, $ZnCl_2$ was added after expression to attempt to solubilize the inclusion bodies. It was thought that this might help to drive the incorporation of Zn^{2+} into the Zn-binding site and facilitate proper protein folding. Samples induced with IPTG (Fig. 7) showed higher expression of DmpLNO compared to samples that were not induced.

Although the oxygenase subunit expression increased, the protein mainly remained as inclusion bodies when comparing the supernatant and cell pellet samples by SDS-PAGE analysis (Fig. 7). Furthermore, addition of Zn^{2+} did not solubilize any portion of what was in the pellet. The lack of success in these experiments, and others in the lab, in obtaining adequate amounts of variant proteins of the oxygenase indicated that another approach for studying the Zn^{2+} -binding site of phenol hydroxylase component was required.

Removal of Zn^{2+} from the cysteine-coordinated site might be achieved using a combination of denaturants, reducing agents and chelating agents. Various combinations of these reagents were attempted, along with dialysis or other methods of desalting. The metal content was analysed by inductively-coupled plasma mass spectrometry (ICP-MS) to verify the success of metal removal.

As a reference point for these experiments, oxygenase was first studied to follow secondary and tertiary structural changes with thermal denaturation using far-UV circular dichroism (far-UV CD) and fluorescence spectroscopies, respectively. The secondary structure of the oxygenase (DmpLNO) is mainly α -helical, as observed in the crystal structure of the orthologue from *Pseudomonas* sp. OX1 that has 78% sequence identity to oxygenase in *Pseudomonas* sp. CF600^{Error! Bookmark not defined.}. In the far-UV CD spectra collected for DmpLNO at a temperature of 25 °C, there are two peak signals at 222 and 208 nm, which are characteristic of α -helices⁶⁷. At 95 °C, there is loss of α -helical structure in the wild-type protein as indicated by the denaturation curve (Fig. 8B) and the loss of ellipticities at 222 and 208 nm (Fig. 8A). Visible insoluble protein was observed in the sample solution after this experiment was completed, consistent with irreversible denaturation of the protein.

Thermal denaturation of the oxygenase was also measured using fluorescence spectroscopy with an excitation wavelength of 280 nm, and monitoring the emission spectra of tryptophan and tyrosine residues. ICP-MS results of the native oxygenase preparations used showed an average of $4.0 \pm 0.5 \text{ Fe}^{2+}$ /mole of protein and $2.5 \pm 0.5 \text{ Zn}^{2+}$ /mole protein, which is similar to previous studies³⁵,[Error! Bookmark not defined.](#)

As the temperature increased, a decrease in fluorescence intensity was observed, together with a red-shift to 347 nm from the initial wavelength maximum at 337 nm. Unfolding of the protein structure exposes the aromatic residues to the hydrophilic environment, hence lowering the quantum yield of the residues and shifting the spectrum to longer wavelengths.

Various reagents, including thiol reagents, chelators and denaturants, were tested for their ability to remove Zn^{2+} from the oxygenase. Tests were first performed by incubating the oxygenase with a reducing agent, dithiothreitol (DTT) that is small in size, a relatively good reductant and is capable of forming a complex with zinc⁶⁸, followed by dialysis against metal-free buffer. A reducing agent would keep the cysteine sulfur groups in the thiol form, and that may help in removing Zn^{2+} , or at least prevent the cysteine residues from oxidizing when Zn^{2+} is removed. As shown by the ICP-MS results (Table 2), the zinc content did not decrease after such a treatment.

Ethylenediamine tetraacetic acid (EDTA) is a chelator that has high affinity for Zn^{2+} and Fe^{2+} : it was added together with DTT to see if the two reagents together could remove the metals. The reducing agent can keep the protein thiol groups reduced, while EDTA could potentially sequester Zn^{2+} from the oxygenase. The ICP-MS results pre- and post-dialysis show that both zinc and iron contents are unchanged by this treatment (Table 3).

In response to temperature, as monitored by far-UV CD and fluorescence spectroscopies, all pre-dialysis EDTA/DTT samples appeared to undergo loss of structure in a manner similar to untreated oxygenase (Figs. 10A & 11, respectively). As seen from using CD spectroscopy, the post-dialysis samples after heating at 95 °C showed incomplete denaturation. The denaturation profile monitored at 222 nm shows T_m values of 52 and 50 °C for both EDTA and EDTA/DTT treated samples, respectively, and the signal plateaued well before it reached anywhere near zero mdeg. α -Helix to β -sheet transformations are common among many α -helical proteins whether it is due to chemical, pH or temperature change⁶⁹. Although the oxygenase subunit of phenol hydroxylase fits the criteria of being mainly α -helical and has more than the minimum number of amino acids required for the α - β transition, it is difficult to determine if this transition is happening to the structure upon increasing temperature since ellipticity at 208 nm becomes obscured by the background noise.

Tris(2-carboxyethyl)phosphine (TCEP) is an effective reductant that contains no thiol groups, but is very effective in keeping disulfide bonds reduced in both acidic and basic conditions, unlike DTT which easily oxidizes around neutral pH⁷⁰. Treatment by TCEP alone or in combination with EDTA was examined, and all post-dialysis samples also failed to denature completely after heating to 95 °C as shown in the CD spectra (Fig. 12), similar to the post-dialysis preparations treated with EDTA and DTT. Complete unfolding and denaturation of the oxygenase protein occurred with samples only prior to buffer exchange using dialysis.

From the two sets of experiments (EDTA/DTT and EDTA/TCEP treatments), post-dialysis denaturation data indicated that dialysis of the samples is likely the cause of a structural

change in the protein that results in incomplete unfolding, unlike the native enzyme or pre-dialysis samples which show complete unfolding.

As with the EDTA-treated and DTT-treated samples, ICP-MS results for the TCEP-treated oxygenase showed that Zn^{2+} is not removed from the enzyme, and there is also very little loss of iron. Therefore, the structural changes that are implied by the inability to completely denature the enzyme after these treatments do not appear related to metal ion removal.

The possibility that a protein denaturant such as urea could help to remove metal ions from the oxygenase was examined. Addition of urea (5 M) to EDTA/DTT treated oxygenase followed by dialysis gave an ICP-MS result that showed lowered zinc content in the pre- to post-dialysis samples, from 1.9 to 0.1 Zn^{2+} per mol protein, and iron content was also affected with values decreasing from 4.0 to 0.1 Fe^{2+} per mol protein when compared to the untreated protein. The concentration of 5 M is high, so it is expected that the protein would unfold completely, consistent with the observation that the CD signal decreases from -25 mdeg in the native enzyme to -9 mdeg at 5 M urea at 222 nm (Fig. 14). Loss of metal ions would be expected for completely unfolded protein, and would be removed by buffer exchange. However, if possible, it would be preferable not to completely unfold the enzyme but instead perturb the structure enough to facilitate metal ion removal. Thus, a test was performed using oxygenase incubated with varying concentrations of urea (0 to 8 M, Figs. 14A & B) to determine the minimum amount of urea that might perturb the structure of the oxygenase without significant unfolding. As is shown in Fig. 14A, 0.5 M urea appeared to be a suitable concentration that did not alter the α -helical structure much. Inclusion of 0.5 M urea was further tested in experiments to remove metal ions.

Tetrakis-(2-Pyridylmethyl)ethylenediamine (TPEN) is a chelator that has been used for intracellular chelation of zinc⁶³. It was used, together with DTT in the presence and absence of urea, followed by dialysis, to attempt Zn²⁺ removal from the oxygenase. ICP-MS results showed successful removal of Fe²⁺ and Zn²⁺ in the presence of urea/DTT/TPEN with the metal content decreasing from 4.0 mol Fe²⁺ and 2.5 mol Zn²⁺ to 0.3 and 0.1 mol iron and zinc, respectively, per mol of oxygenase (Table 7). In the absence of urea, the Zn²⁺ content of 1.3 mol/mol oxygenase was significantly higher than when urea was present, and Fe²⁺ was at 0.1 mol/mol oxygenase. Thus, urea is required in combination with the chelator and reducing agent, followed by dialysis, for the most effective removal of Zn²⁺.

In the pre- and post-dialysis CD spectra of TPEN/DTT/urea treated oxygenase (Fig. 17A & B), the structure of the protein changes as indicated by the apparent loss of signal at 208 nm at 25 °C and the protein completely denatures/precipitates out of the solution at 95 °C. Thermal denaturation of these samples indicates that the protein is unfolded by 95 °C (Fig. 17C). What is interesting to note here is the T_m value (transition midpoint temperature) of the post-dialysis preparation at 62 °C, which is somewhat higher than that of the native enzyme (57 °C). Also, it has a T_m that is 12 to 13 °C higher compared to all previous post-dialysis samples (EDTA, EDTA/DTT, TCEP and TCEP/EDTA treatment), which may indicate an increase in stability of the protein. Fluorescence data (not shown) has indicated that the starting wavelength maxima at 25 °C are at 341 and 343 nm for pre- and post-dialysis samples, respectively, compared to 336 or 338 nm for untreated samples, indicating the protein structure is already partially unfolded after TPEN/DTT/urea treatment, exposing the aromatic residues to the hydrophilic environment. However, the fluorescence intensities of both samples are quite different, as the spectrum of

post-dialysis sample starts at intensity twice as high compared to that of pre-dialysis sample (Fig. 18).

Although dialysis is a method that is effective at reagent removal, it is a lengthy process and requires treatment of large buffer volumes with an expensive metal chelating resin. Column-based buffer exchange was thus tested as an alternative to dialysis. The first set of experiments used a NAP-5 column (GE Healthcare) to remove reagents after the oxygenase was treated with the chelator, EDTA, in the presence or absence of DTT (see *Materials and Methods*). Results of thermal denaturation as monitored by Far-UV CD and fluorescence spectroscopies mirrored those of the equivalent experiment performed using dialysis to remove EDTA and DTT. Metal analysis of samples after the NAP-5 column step confirmed that Zn^{2+} was not successfully removed, but there was significant loss of iron (Table 6).

Another column-based procedure was a mini-Chelex[®] column, whose resin can bind metal ions. Thus, oxygenase samples that had been treated with DTT, TPEN/DTT, DTT/urea or EDTA/DTT/urea were passed through a Chelex[®] column, and then tested for metal content (Table 8). ICP-MS showed that the most efficient combination was TPEN/DTT treatment, followed by Chelex chromatography, resulting in 0.1 mol of zinc and iron per mol of oxygenase. The other three samples had roughly the same zinc content, averaging 1.2 mol/mol oxygenase, so TPEN and DTT are most effective at removing Zn^{2+} from the oxygenase.

CONCLUSIONS

The inability to successfully express variants of DmpLNO oxygenase where any of the Zn^{2+} -binding ligands had been substituted suggests that this metal ion plays a role in stabilizing the protein structure. The results presented in this thesis indicated that a combination of the Zn^{2+} chelator, TPEN, the reductant, DTT, and a low concentration the protein denaturant, urea, followed either by dialysis or a Chelex column, effectively removed both zinc and iron. The spectroscopic experiments indicated that these samples had altered CD and fluorescence spectra, but the thermal denaturation experiments indicated that the apo-protein stability was similar to that of the holo-protein samples.

FUTURE WORK

Although removal of Zn^{2+} from the oxygenase was accomplished, Fe^{2+} was also removed from the enzyme. In order to study the role of Zn^{2+} , it is necessary to have a preparation that has an intact binuclear iron centre. Accordingly, future studies should include the addition of Fe^{2+} to the apo-enzyme, using procedures that have already been developed³⁵. The activity of the enzyme before and after the addition of Zn^{2+} would be monitored. Secondary and tertiary structure in the presence and absence of Zn^{2+} would be examined using circular dichroism and fluorescence spectroscopies, and protein stability would be probed by thermal or chemical denaturation studies.

The importance of individual residues in the Zn^{2+} binding site could be best probed by characterizing variants of the oxygenase. However, work with variant proteins that were generated in the present study proved it was difficult since the proteins were found exclusively in the particulate fraction with the formation of inclusion bodies. There are published protocol methods available to purify proteins expressed in inclusion bodies. These include solubilization of the inclusion bodies by using denaturants (GdHCl or urea) or detergents (SDS)⁷¹ and then refolding the protein in the presence and absence of Zn^{2+} to recover the variant enzyme. Refolding the enzyme under study may be difficult, however, because of the many subunits it possesses. If this approach were successful, the variant proteins can be tested for enzyme activity, structural changes and stability to probe the roles of variants with alterations of amino acids at the Zn^{2+} binding site.

REFERENCES

-
- ¹ Krastanov, A., Alexieva, Z., and Yemendzhiev, H. (2013) *Eng. In Life Sci.* 13, 76-87.
- ² Berg, J.M., Tymoczko, J.L., and Stryer, L. (2006) Chapter 35: Drug Development, *Biochemistry 6th ed.* (pp. 1001-1026). New York: W. H. Freeman and Company.
- ³ Deichmann, W.M.B., and Witherup, S. (1944) *J. Pharmacol. Exp. Ther.* 40, 233-240.
- ⁴ <http://www.hc-sc.gc.ca/ewh-semt/pubs/contaminants/psl2-lsp2/phenol/index-eng.php> Accessed Feb. 16, 2014.
- ⁵ Conning, D.M., and Hayes, M.J. (1970) *Brit. J. Industr. Med.* 27, 155-159.
- ⁶ Brown, V.K.H., Box, V.L., and Simpson, B.J. (1975) *Arch Environ Health* 30, 1-6.
- ⁷ Kumar, S., Mishra, V.K., Kumar, U., Kumar, A., and Varghese, S. (2013) *Intl. J. Agric. Env. Biotech.* 6, 39-44.
- ⁸ Souidi, M.R., and Kolahchi, N. (2011) *Prog. In Biol. Sci.* 1, 31-40.
- ⁹ http://inchem.org/documents/hsg/hsg/hsg88_e.htm Accessed Feb. 16, 2014.
- ¹⁰ Medel, A., Bustos, E., Esquivel, K., Godínez, L.A., and Meas, Y. (2012) *Intl. J. of Photoenergy* 2012, 1-6.
- ¹¹ Mrozik, A., Miga, S., and Piotrowska-Seget, Z. (2011) *J. Appl. Microbiol.* 111, 1357-1370.
- ¹² Alexander, M., and Lustigman, B.K. (1966) *J. Agr. Food Chem.* 14, 410-413.
- ¹³ MacRae, I.C., and Alexander, M. (1965) *J. Agr. Food Chem* 13, 72-76.
- ¹⁴ Alexander, M., and Aleem, I.H. (1961) *Agri. Food and Chem.* 9, 44-47.
- ¹⁵ Dagley, S., and Patel, M.D. (1957) *Biochem. J.* 66, 227-233.
- ¹⁶ Bayly, R.C., Dagley, S., and Gibson, D.T. (1966) *Biochem J.* 101, 293-301.
- ¹⁷ Powlowski, J., and Shingler, V. (1994) *Biodegradation* 5, 219-236.
- ¹⁸ Feist, C.F., and Hegeman, G.D. (1969) *J. Bacteriol.* 100, 869-877.
- ¹⁹ Sala-Trepat, J.M., and Evans, W.C. (1971) *Eur. J. Biochem.* 20, 400-413.

-
- ²⁰ Hughes, E.J., Bayly, R.C., and Skurray, R.A. (1984) *J. Bacteriol.* 158, 79-83.
- ²¹ Neujahr, H.Y., and Varga, J.M. (1970) *Eur. J. Biochem.* 13, 37-44.
- ²² Gaal, A., and Neujahr, H.Y. (1979) *J. Bacteriol.* 137, 13-21.
- ²³ Cain, R.B., Bilton, R.F., and Darrah, J.A. (1968) *Biochem. J.* 108, 797-828.
- ²⁴ Neujahr, H.Y., and Gaal, A. (1973) *Eur. J. Biochem.* 35, 386-400.
- ²⁵ Neujahr, H.Y., Lindsjö, S., and Varga, J.M. (1974) *Antonie van Leeuwenhoek J. Microbiol. Serol.* 40, 209-216.
- ²⁶ Dagley, S. (1971) *Adv. Microb. Physiol.* 6, 1-46.
- ²⁷ Ornston, L.N., and Stanier, R.Y. (1966) *J. Biol. Chem.* 241, 3776-3786.
- ²⁸ Ornston, L.N. (1966) *J. Biol. Chem.* 241, 3787-3794.
- ²⁹ Ornston, L.N. (1966) *J. Biol. Chem.* 241, 3795-3799.
- ³⁰ Ornston, L.N. (1966) *J. Biol. Chem.* 241, 3800-3810.
- ³¹ Antai, S.P., and Crawford, D.L. (1983) *Can. J. Microbiol.* 29, 142-143.
- ³² Nordlund, I., Powlowski, J., and Shingler, V. (1990) *J. Bacteriol.* 172, 6826-6833.
- ³³ Powlowski, J., and Shingler, V. (1990) *J. Bacteriol.* 172, 6834-6840.
- ³⁴ Cadieux, E., Vrajmasu, V., Achim, C., Powlowski, J., and Münck, E. (2002) *Biochemistry* 41, 10680-10691.
- ³⁵ Cadieux, E. (2002) Chapter 3: The role of DmpK in the assembly of the binuclear iron center in phenol hydroxylase, *Characterization of phenol hydroxylase and its auxiliary proteins, dmpM and dmpK, from Pseudomonas sp. strain CF600* (pp. 99-147). Montreal, Canada: Concordia University.
- ³⁶ Powlowski, J., Sealy, J., Shingler, V., and Cadieux, E. (1997) *J. Biol. Chem.* 272, 945-951.
- ³⁷ Sazinsky, M.H., Dunten, P.W., McCormick, M.S., DiDonato, A., and Lippard, S.J. (2006) *Biochemistry* 45, 15392-15404.
- ³⁸ Badger, M.R., and Price, G.D. (1994) *Annu. Rev. Plant Physiol. Plant Mol. Biol.* 45, 369-392.
- ³⁹ Keilin, D., and Mann, T. (1939) *Nature* 144, 442-443.

-
- ⁴⁰ Christianson, D.W. (1991) *Adv. Protein Chem.* 42, 281-355.
- ⁴¹ Williams, R.J.P. (1987) *Polyhedron* 6, 61-69.
- ⁴² McCall, K.A., Huang, C.C., and Fierke, C.A. (2000) *Am. Soc. Nutri. Sci.*, 1437S-1446S.
- ⁴³ Bertini, I., Luchinat, C., and Monnanni, R. (1985) *J. Chem. Edu.* 62, 924-927.
- ⁴⁴ Vallee, B.L., and Auld, D.S. (1990) *Proc. Natl. Acad. Sci. USA* 87, 220-224.
- ⁴⁵ Christianson, D.W., and Cox, J.D. (1999) *Annu. Rev. Biochem.* 68, 33-57.
- ⁴⁶ Lovejoy, B., Cleasby, A., Hassell, A.M., Longley, K., Luther, M.A., Weigl, D., McGeehan, G., McElroy, A.B., Drewry, D., Lambert, M.H., and Jordan, S.R. (1994) *Science* 263, 375-377.
- ⁴⁷ Reichard, P., and Hanshoff, G. (1956) *Acta Chemica Scandinavica* 10, 548-566.
- ⁴⁸ Klug, A., and Schwabe, J.W. (1995) *FASEB* 9, 597-604.
- ⁴⁹ Vallee, B.L., and Auld, D.S. (1990) *Biochemistry* 29, 5647-5659.
- ⁵⁰ Chesters, J.K. (1972) *Biochem. J.* 130, 133-139.
- ⁵¹ <http://pfam.sanger.ac.uk/family/PF04945> Accessed Sept. 16, 2013.
- ⁵² Sonnhammer, E.L.L., Eddy, S.R., and Durbin, R. (1997) *Proteins* 28, 405-420
- ⁵³ Bateman, A., Birney, E., Cerruti, L., Durbin, R., Etwiller, L., Marshall, M., and Sonnhammer, E.L.L. (2002) *Nucleic Acids Res* 30, 276-280.
- ⁵⁴ Powlowski, J., and Shingler, V. unpublished manuscript
- ⁵⁵ Brown, R.E., Jarvis, K.L., and Hyland, K.J. (1989) *Anal. Biochem.* 180, 136 – 138.
- ⁵⁶ Cadieux, E. and Powlowski, J. (1997) *J. Biol. Chem.* 272, 945-951.
- ⁵⁷ Wong, A. unpublished data.
- ⁵⁸ Cadieux, E. (2002) Chapter 4: Properties of a novel multicomponent phenol hydroxylase encoded by the *dmp* operon of *Pseudomonas* sp. strain CF600, *Characterization of phenol hydroxylase and its auxiliary proteins, dmpM and dmpK, from Pseudomonas* sp. strain CF600 (pp. 148-209). Montreal, Canada: Concordia University.

-
- ⁵⁹ Lei, Yu. (2008) Chapter 4: Active site studies and metal ion requirements of DmpG, an aldolase involved in bacterial degradation of aromatic compounds, Active site studies of DmpFG a bifunctional aldolase/dehydrogenase from *Pseudomonas* sp. strain CF600 (pp. 130). Montreal, Canada: Concordia University.
- ⁶⁰ Wrolstad, R.E., Acree, T.E., Decker, E.A., Penner, M.H., Reid, D.S., Schwartz, S.J., Shoemaker, C.F., Smith, D.M., and Sporns, P. (2005) *Handbook of food analytical chemistry water, proteins, enzymes, lipids and carbohydrates*. John Wiley & Sons, New Jersey, pp. 262.
- ⁶¹ Lakowicz, J.R. (2006) *Principles of Fluorescence Spectroscopy* 3rd ed. Springer Science & Business Media, New York, pp. 205-207.
- ⁶² Méplan, C., Richard, M.J., and Hainaut, P. (2000) *Oncogene* 19, 5227-5236.
- ⁶³ <http://www.piercenet.com/product/tcep-hcl> Accessed Nov. 24, 2013
- ⁶⁴ Arslan, P., Di Virgilio, F., and Beltrame, M. (1985) *J. Biol. Chem.* 260, 2719-2727.
- ⁶⁵ Jakob, U., Eser, M., and Bardwell, J.C.A. (2000) *J. Biol. Chem.* 275, 38302-38310.
- ⁶⁶ www.ebi.ac.uk/interpro/protein/P19732 Accessed Dec17 2013
- ⁶⁷ Corrêa, D.H.A., and Ramos, C.H.I. (2009) *African Journal of Biochemistry Research* 3, 164-173.
- ⁶⁸ Cornell, N.W., and Crivaro, K.E. (1972) *Anal. Biochem.* 47, 203-208.
- ⁶⁹ Qin, Z., and Buehler, M.J. (2010) *Phys. Lett. Rev.* 104, 198304-1-198304-4.
- ⁷⁰ Han, J.C., and Han G.Y. (1994) *Anal. Biochem.* 220, 5-10.
- ⁷¹ Sambrook, J., and Russell, D.W. (2001) *Molecular cloning: a laboratory manual* (vol. 3) 3rd ed. Cold Spring Harbor, New York, pp.15.49-15.54.